Dissertation

Thresholdless electrooptical mode in Ferroelectric Liquid Crystals

Vom Fachbereich Physik
der Technischen Universität Darmstadt

zur Erlangung des Grades
eines Doktors der Naturwissenschaften
(Dr. rer. nat.)

genehmigte Dissertation von
Dipl.-Phys. Fedor V. Podgornov
aus Korkino, Rußland

Referent: Prof. Dr. T. Tschudi
Korreferent: Prof. Dr. W. Haase (FB 7)

Tag der Einreichung: 11. 02. 2004
Tag der Prüfung: 19. 04. 2004

Darmstadt 2004

D17

Contents

Introduction

Nowadays, we are the witnesses of the rapid growth of interest to both fundamental research and application development in the field of liquid crystals (LC's). These material attract considerable attention due to their unique physical properties, such as the combination of the fluidity and the orientational/positional ordering, strong sensitivity to the electrical/magnetical fields, mechanical stresses, *etc.* The electrooptical properties of LC's allow to utilize liquid crystals in devices like liquid crystal displays (LCD's), switchers, deflectors, *etc*.

In this connection, investigation of the electrooptical effects in LC's plays a crucial role not only for the fundamental research but also for their application.

Among all liquid crystals, the most usable and the most investigated type are nematic liquid crystals (NLC's), which were discovered more than a century ago. NLC's are characterized by the orientational ordering and absence of the positional ordering of the constituting molecules. Due to symmetry reasons, nematics are macroscopically non-polar. As the result, they are not sensitive to the polarity of the applied electric field and have slow response time laying in millisecond range. Presently, many electrooptical modes of NLC's are known: S-effect, B-effect, twist and supertwist NLC's, the transient nematic effect, the dual frequency NLC's [Blinov]. Despite, practically all commercially available LC devices are based on NLC's, the problem with the response time is still not solved.

However, about 28 years ago, a new type of liquid crystals was discovered, namely, chiral smectic C (SmC*) - Ferroelectric Liquid Crystals (FLC's) [Meyer]. The remarkable properties of the FLC's are their orientational and one dimensional positional ordering as well as chirality of the molecules, which result in the existence of the *macroscopical* dipole moment. The latter circumstance has three very important consequences for optical applications: 1) dependence of the electrooptical response on the polarity of the applied electric field, 2) fast response time (laying in microsecond range), and 3) in-plane switching of the FLC director [Lwall]. In other words, the FLC's can be considered as a competitor of NLC's for utilization in applications. Hence, it is very important to investigate the electrooptical properties of the FLC's.

Since discovering of the FLC's, several electrooptical modes were found: Surface Stabilized Ferroelectric Liquid Crystal (SSFLC) [LagClar], Deformed Helix Ferroelectric Liquid Crystal (DHFLC) [BerSha], and, so-called, the V-shaped switchable (thresholdless mode) FLC [Inui].

The overview of the main electrooptical modes in FLC's will be given in chapter №1. Of the present thesis.

Among all electrooptical effects in FLC's, the most attractive modes are DHFLC and V-shaped FLC. These effects can provide a continuous gray scale. At the same time, only the V-shape mode demonstrates the thresholdless switching. Utilization of this effect in active matrix displays can greatly simplify the fabrication process and improve their performance.

However, since discovering of the V-shaped mode, its nature is still a subject of controversial discussion.

Up to now, several explanations of the nature of this mode were proposed, namely 1) the collective motion model based on the assumption that V-shaped switching is an inherent property of the Sm X^* mesophase [Inui, Fukuda]; 2) electrostatic approach suggested by N. Clark *et al.* [ClarCol,Cop,MacClar], where "stiffening" of the polarization field by its charge self-interaction causes the FLC to reorient as a uniform block; 3) the strong polar anchoring model of FLC's or AFLC's to the alignment layers [Elst1, Elst2].

However, despite strong affords, the earlier work did not reveal the origin of the V-shaped switching. Therefore, further investigation of the nature of this mode is absolutely necessary.

A new approach was proposed recently by L. Blinov, W. Haase, S. Pikin, *et al* [Blm1, Blm2]. The principal idea is the key role of the dynamic voltage divider formed by the basic elements of the cell, namely the alignment layer and the liquid crystal. Due to this divider, the voltage on the FLC layer is radically different from those on the entire cell. The transmittance plotted as a function of the total voltage applied to the cell is different from that as a function of the real voltage on the FLC layer. Only, in the former case, the V-shaped curve is observable. In other words, the V-shaped switching is not a real but rather an apparent effect. Utilizing this approach, cells with inversion frequency higher than 700 Hz could be

realized. On the other hand, in papers [Blm3, Blm4], using computer simulations, the influence of material parameters of the FLC mixtures on the performance of the V-shape mode was revealed.

In chapter №2, FLC materials, cell assembling technique, experimental setup and the structure of the modeling software necessary for the investigation of this new electrooprical mode will be presented.

In chapter №3, this thresholdless mode will be described. The nature of the thresholdless hysteresis free switching will be discussed in details and the influence of different contributions to the inversion frequency (capacitance of the alignment layers, the FLC conductivity, the spontaneous polarization, anchoring conditions) in framework of the dynamic voltage divider model will be demonstrated.

In chapter №4, the optimized modulators based on the V-shaped switching mode as well as their gray scale performance will be demonstrated. The experimentally obtained data will be compared with computer modeling.

Aims of the work

- **Investigation of the mechanism of the V-shaped switching mode in Feroelectric Liquid Crystals and computer modeling:**
  a) Role of the dynamic voltage divider formed by a FLC cell structure for V-shaped switching performance.
  b) The role of the spontaneous polarization, polar anchoring energy and the FLC texture on V-shaped switching.
  c) Influence of the FLC conductivity on the inversion frequency of the cells.
  d) Investigation of the gray scale capabilities of V-shaped switching mode.

Chapter №1

Electrooptical effects in Ferroelectric liquid crystals

1.1 Liquid crystals

Liquid crystals are the intermediate state (mesophase) between the crystalline solid and amorphous liquids.

A substance in this state is strongly anisotropic in some of its properties and yet exhibits a certain degree of fluidity, which in some cases can be compared to that of an ordinary liquid.

Mesomorphism occurs in substances which molecules are highly geometrically anisotropic in shape, like a rod or a disc. Depending on the molecular structure, the system can pass through one or more mesomorphic states before it is transformed in to the isotropic liquid. Transitions to these intermediate states may induced by purely thermal process (thermotropic) or by the influence of the solvents (lyotropic). By the internal structure, the thermotropic liquid crystals can be subdivided on nematics and smectics.

1.1.1 Nematic liquid crystal

Nematic liquid crystals are characterized by long-range orientational order and the absence of long range positional order of the molecules [Blinov, Jeu]. As in the case of the isotropic matter, the density does not depend on the coordinates, $\rho(r) = \text{const}$. The director in nematics satisfies the condition **n**=-**n** and coincides with the direction of the optical axis (see Fig. 1.1 a).

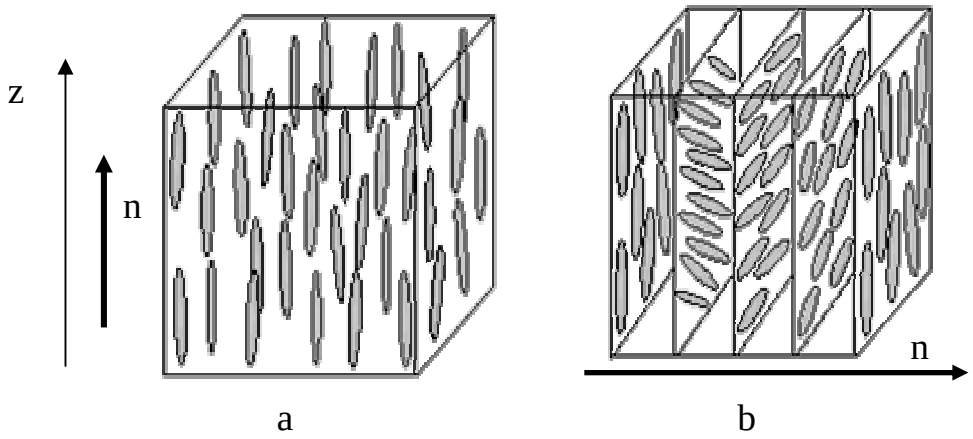

Figure 1.1 : a) structure of the nematics; b) structure of the chiral nematics (cholesterics). n is the director, z is the long axis

The nematic phase is cylindrically symmetric with respect to the optical axis and has mirror symmetry with respect to the plane perpendicular to *z*. In other words nematics have the point symmetry group $D_{\infty h}$, which prohibits the existence of the macroscopical dipole moment. As a rule, the phase transition from the isotropic phase into the nematics is a weak first order transition [Blinov] with a small jump in the order parameter S and other thermodynamic properties. One can also observe the temperature divergence in some physical parameters (e.g. heat capacitance, dielectric permittivity) in the pretransitional region.

Conventional nematic liquid crystals formed by rod-like molecules constitute a uniaxial medium with nonpolar symmetry. Due to this remarkable property of the nematics is possible to create a uniform orientation of the molecular axes throughout the sample, thus obtaining a monodomain sample.

If one add chiral molecules to the nematics or use chiral mesogenic molecules one can get the so called cholesteric mesophase [BelSon]. Cholesterics are characterized by the fact that the direction of the long molecular axes in each neighboring layer is rotated at some angle with respect to the molecules in the preceding layer. As the result, a helix is formed (see Fig. 1.1 b). The helical pitch depends on the nature of the molecules. Corresponding to the pitch, the axis of orientation of the molecules rotates through an angle 2π, although the period of the optical properties is equal to π. Locally, like nematics, cholesterics are uniaxial. On the macroscopical scale, due to averaging, the helical structure is also uniaxial, the optical axis coinciding with the helical axis which is perpendicular to the local (nematic) optical axis. The remarkable optical property of the cholesterics is the selective reflection of the light. The wavelength of the reflected light is a function of the helical pitch.

1.1.2 Smectic liquid crystals

The other class of liquid crystals are smectics where the molecules do exhibit a degree of positional ordering [Elston, Blinov, Lwall]. In the most important smectic phases (SmA, SmC), this positional ordering is in one dimension only, forming layers of two-dimensional nematis. The most simple smectic phase is the

smectic A (SmA) phase (see Fig. 1.2 a), in which the direction of the averaged molecular orientation is along the smectic layer normal. In addition, there is a family of tilted smectic liquid crystal phases, in which the director is at a fixed angle θ with respect to the layer normal. Out of them, the simplest case is the smectic C (SmC), see figure 1.2 b.

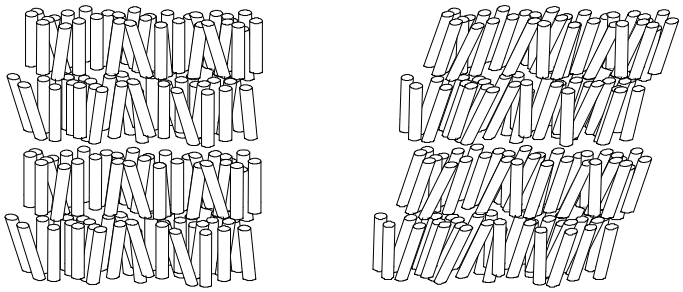

Figure1 .2: Structure of the smectics a) Smectic A (SmA), b) Smectic C (SmC)

When the phases comprise chiral molecules, the chiral versions of these phase are formed: SmA^*, SmC^*. One of the effect of the chirality of the molecules in the case of the tilted smectic SmC^* is to cause the azimuthal angles of the director to precess slowly from one layer to the next. This creates a macroscopic helical structure with its axis along the layer normal (see Fig. 1.3).

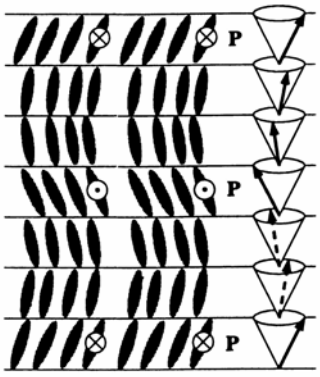

Figure 1.3 : Structure of the chiral smectic C* phase

Like the orientational ordering in nematics, the positional ordering of smectics is not perfect. In some cases a plot of the density of the molecular centers of mass as a function of distance along the normal to the layers follows a sinusoidal law [Lwall]:

$$\rho(x) = \rho_0(1 + \psi \sin(\frac{2\pi x}{\delta})),$$

where ρ_0 is the mean density and δ is the layer spacing, which are typically a few nanometers. ψ is the smectic order parameter, which is the ratio of the amplitude of oscillation to the mean layer density.

Inside each layer, the orientational ordering with respect to director is described by a nematic order parameter:

$$S = \left\langle \frac{3}{2}\cos^2 \vartheta - \frac{1}{2} \right\rangle.$$

Here ϑ is the angle between the molecule and the director.

Order parameters S and ψ are sufficient to describe the SmA phase. But in case

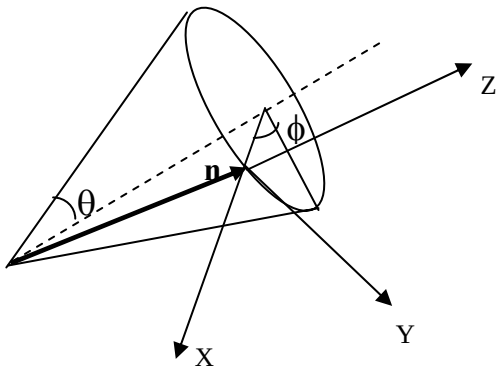

Figure 1.4: Arrangement of smectic C liquid crystal molecule

of the tilted smectic phases, two further order parameters are required for the description of the phase, namely, the azimuthal angle ϕ of the director with respect to the fixed coordinate system and the tilt of the director with respect to the layer normal θ (see Fig. 1.4).

Point symmetries of the smectic phases and ferroelectricity

In addition to the translation symmetry, the smectic A phase the following point symmetry (Elston, Lwall):

a) mirror symmetry in any plane parallel to the smectic layers that is either exactly between the planes or the midplanes
b) two fold rotational symmetry around any axis lying within any of the above mentioned mirror planes
c) mirror symmetry in any plane perpendicular to the smectic layers
d) complete rotational symmetry about the axis perpendicular to the layers.

This set of point symmetries corresponds to the point symmetry $D_{\infty h}$ in the Schoenflies notation. The chiral version of the SmA phase (SmA^*) has only the rotational symmetries, the mirror symmetries no longer exist because the molecules are chiral. This reduces the symmetry of the SmA^* phase to D_∞. The high symmetry of the SmA and SmA^* phases precludes the existence of any net spontaneous polarization, just like in nematics. Therefore, they can only respond to an applied electric field via an induced electric dipole. In contrast to SmA, SmC liquid crystals have the following point symmetries:

a) mirror symmetry in the tilt plane of the molecules
b) two fold rotational symmetry about the axis perpendicular to the tilt plane of the molecules, either exactly between layers or exactly mid-layer.

This combination corresponds to the C_{2h} point symmetry group in the Schoenflies notation, and also excludes the existence of any net spontaneous polarization in the SmC liquid crystalline phase. However, in the chiral version of the SmC phase, the mirror symmetry is no longer present and only the rotational symmetry remains.

The symmetry group is reduced to C_2. It allows the existence of the spontaneous polarization P_S along the C_2 axis of each smectic layer. The net spontaneous polarization arises due to the lack of rotational degeneracy of the molecules about their long axes within the smectic layer. Hence, as predicted by Meyer *et al* [Meyer], SmC^* liquid crystals are ferroelectric.

But this statement is strictly valid for a single smectic layer only. The chirality of the molecules also causes a macroscopic helical structure, such that the C_2 axis (and hence the polarization direction) precesses slowly from one layer to the

next. Thus on a macroscopic level there is no net polarization, and a more correct name for this phase is therefore `helielectric`. However, in a confined cell geometry the helical structure is suppressed (surface stabilization), and then the system is truly ferroelectric.

1.2 Electrooptical effects in Ferroelectric Liquid Crystals

1.2.1 Electroclinic effect

The electroclinic effect is present in chiral SmA* liquid crystals due to the soft mode. In the SmA* phase, the molecules form parallel layers which are perpendicular to the boundary plates, but they do not have spontaneous tilt The term “electroclinic” arises because the application of an electric field induces this tilt. These are also called soft-mode ferroelectric – effect liquid crystals because as the liquid crystal is cooled down to the phase transition SmA*-SmC*, one of the elastic constants vanishes, softening the restoring force which keeps the molecules perpendicular to the smectic layers. Upon application of the electric field the molecules tilt in the plane of the substrate rather than around a tilt cone. The direction of the induced molecular tilt is a function of the polarity of the applied field [Blinov].

The desirable characteristics of the electroclinic liquid crystals are that they exhibit a very fast response time and linear response to an electric field.

The switching time in the electroclinic mode is independent on the strength of the electric field. It depends only on the rotational viscosity γ_φ and the elastic modulus A'.

This time can be obtained analytically from the equation of the balance of the viscous and elastic torques known as the Landau-Khalatnikov equation:

$$\gamma_\varphi \frac{\partial \theta}{\partial t} + A^* \theta = 0 . \qquad 1.5$$

This equation has rather simple solution, namely:

$$\theta = \theta(0)[1 - \exp(-t / \tau_\theta)] ,$$

where $\tau_\varphi = \frac{\gamma_\varphi}{A^*}$ is the characteristic response time 1.6

However, the response time strongly depends on temperature.

Optically, the electroclinic effect relies on the birefringence to modulate light. Because the tilt angle θ is at least a factor of 2 smaller than for FLC’s formed from the same substance, the most available mixtures cannot provide the tilt of 22.5^0 to rotate the optic axis at 45^0 which is required to obtain a $\frac{\pi}{2}$ phase shift.

However, using the multiple-cell technique with an 11.25^0 tilt, large modulation has been achieved.

The other advantages of this effect are the absence of the hystersis of the electrooptical response, which results in continuous grey scale capabilities of the electroclinic light modulators.

1.2.2 Deformed Helix Ferroelectric Liquid Crystal Effect (DH FLC)

Deformed helix ferroelectric liquid crystals effect exists in the smectic C* phase when the thickness of the cell is greater than the helical pitch.

The structure of the DHFLC's is layered, so that, the molecular director in each layer is tilted by an angle θ with respect to the layers normal. This tilt direction precesses due to the molecular chirality around the layer normal forming a helicoidal structure with the pitch p_0. To get more pronounced electro-optic effect the geometry should be planar; that is, the smectic layers are perpendicular to the glass substrates [BerScha].

In the absence of an electric field the azimuth φ varies linearly with the coordinate z perpendicular to the layers: $\varphi=q_0z$ with $q_0=2\pi/p_{0se}$ (see Fig. 1.5*)*. Since spontaneous polarization precesses linearly around z it averages macroscopically the total dipole moment to zero.

When an electric field E is applied parallel to the smectic layers it couples with the ferroelectric polarization in the first order and to the static dielectric tensor in second order. As a result of the coupling, the helix is deformed in such a way, that the molecules tend to align perpendicular to E. Opposing this tendency is the elastic force which tends to keep the layers in the equilibrium, nondistorted configuration, resulting in a complicated profile for $\varphi(z)$. Therefore, the first molecules which align perpendicularly to E are those in the layers near to the planes where $\varphi=\pi, 3\pi, 5\pi,....$, for $E>0$, and near to the planes where $\varphi=0, 2\pi, 4\pi, ...$, for $E<0$. As $|E|$ increases, the number of planes, and hence the size, of the regions where φ is an odd multiple of π for $E>0$ and where φ is an even multiple of π for $E<0$ increases.

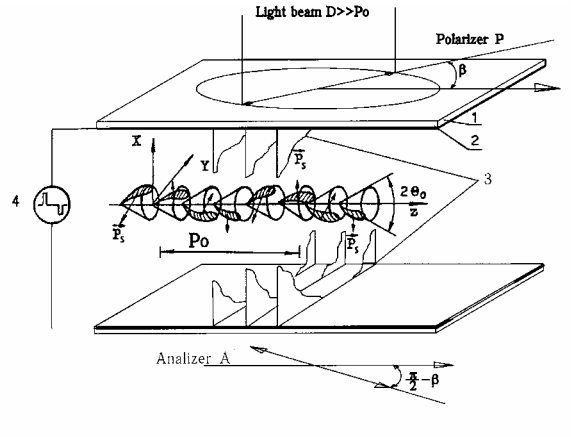

Figure 1.5: The structure of a DH FLC cell [Lwall]: 1 – glass substrates, 2 - transparent conductive electrodes covered by rubbed orienting polymer films, 3- smectic layers, 4 - voltage generator, β - an angle between the polarizer and the helix axis, P_o - helix pitch, *D* - aperture of a light beam.

The size of the regions between the above planes decreases forming walls with thickness $\xi=(K/PE)^{1/2}$ where *K* is an effective elastic constant. The behavior of the helicoidal pitch with E is such that it increases gradually with E until a critical field E_c, where it diverges and the helix is unwound. The helix deformation results in turning the effective optical axis at some angle in the plane of the cell.

Light propagating perpendicular to the helix of a SmC* exhibits unique properties radically different from the case of propagation along the helix or at a small angle to it [Abdulhal].

There are two main effects of the medium on the transmitted light. First of all this is a transformation of the polarization and the second it is the light diffraction. The first is a result of the optical anisotropy, which can be described in terms of the orientation of the optic axis with respect to the incident light polarization and the birefringence.

The light transmittance through the DH FLC cell placed between two crossed polarizers is given by:

$$T(z) = \sin^2\left(\frac{k_0 d}{2}\Delta n(z)\right)\sin^2(2[\Omega(z)+\beta]), \qquad 1.25$$

where k_0 is the wavevector of the incident light, β is the angle between the polarization of the incident light and the z-axis, Ω(z) is the angle between the

projection of the optic axis on the polarizer plane and the z-axis, Δn is the effective birefringence.

The light modulation due to diffraction is a result of the spatial periodicity of the dielectric tensor perpendicular to the propagation direction. The disclination lines which exist in planar samples also contribute to the diffraction [GlogPav]. These lines give rise to dark stripes on the sample separated by the half the helicoidal pitch when viewed under a microscope between crossed polarizers.

According to the numerical solution of the sine-Gordon equation, the switching time should decrease like $\tau \sim \frac{1}{E}$ for intermediate fields and like $\tau \sim \frac{1}{\sqrt{E}}$ for strong electric fields [Abdulmod].

1.2.3 Surface Stabilized Ferroelectric Liquid Crystal Effect (SSFLC)

In 1980 N.Clark and S. Lagerwall [LagerClar] demonstrated that macroscopic polarization could be obtained in smectic C* liquid crystals by suppressing the helix. This is accomplished by constraining the material to fill a region between two plates, which are separated by a distance of less than a few times of the helical pitch.

In an ideal SSFLC the molecules form parallel layers which extended from one boundary plane to the other. This structure is referred as the bookshelf geometry because the layers are next to each other like books in a shelf. The molecules are constrained to move about a tilt cone (see Fig. 1.6)

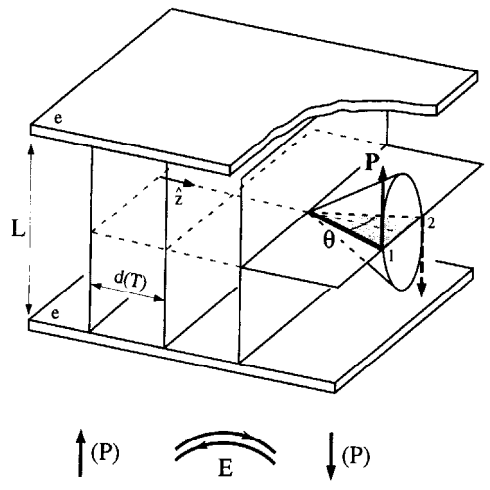

Figure 1.6: Structure of a SSFLC cell

To switch the molecules from one state to the other requires charge of $2P_s$, where P_s is the spontaneous polarization. Additional charge is required to produce a voltage across the plate, which bound the FLC, as with any capacitor. Thus the total charge required to switch an FLC is $2P_s+CV$, where V is the change in the applied voltage and C is the capacitance of the cell.

The dynamics of the switching in SSFLC cells can be described by the equation of the torque balance known as the sine-Gordon equation.

The general solution to equation (1.18) has the form:

$$\varphi(t) = 2\arctan(\tan\frac{\varphi_0}{2}e^{-t/\tau}) . \qquad 1.19$$

Here φ_0 is the angle between E and P_s at time t=0. $\tau = \frac{\gamma_\varphi}{P_s E}$ is the characteristic (response time). This time is inversely proportional to the applied electric field, instead of being inversely proportional to the square of the field as in nematic case. It means that the electrooptical response of the FLC's is faster than that of nematics. The unique advantage of the FLC is the switching is equally fast in both directions, which can be not achieved in nematics.

The transmission of the SSFLC cell placed between two crossed polarizers upon applying electric field can be written as:

$$T = \sin^2 4\theta \sin^2 \frac{\pi d\Delta n}{\lambda} \qquad 1.21$$

where d is the thickness of a cell, λ is the wavelength. The first term is a function of the tilt angle of the FLC mixture. The second term is an oscillatory function of the cell thickness and the wavelength. From this formula, it is easy to see that, for the thinnest cells meeting the halfwavelength condition, their optical performance is close to achromatic.

Bistability of the SSFLC switching

The existence of two thermodynamically stable states with different optical transmission is an important feature of the SSFLC. Several approaches to explain the nature of the bistability in FLC's are known.

First of all, to form a bistable SSFLC cell, ideally the surface alignment should constrain the molecules to be parallel to the boundary planes, but allow the molecular director to rotate freely on this plane [LagerClar].

Insulating alignment layers degrade the bistability. The cause for this is the following. When a voltage is applied to the cell, a field is dropped across the SSFLC and the alignment layers, causing the molecular dipoles to become oriented such that their polarity is opposite to that of the applied field. This can be considered as a net charge created at the interface between the alignment layers and the liquid crystal which is opposite in polarity to that of the adjacent electrode. When the voltage across the cell is switched to zero by shorting the two electrodes together, however, initially the interface charge remains. It produces a field across the SSFLC, which is opposite in polarity to that originally produced by the applied voltage. This *depolarization field* tends to switch the SSFLC away from its saturated orientation. The larger the spontaneous polarization of the SSFLC, the greater the density of interface charge is, resulting in a larger depolarization effect [Modd].

The solution to this problem is to use conductive alignment layers [ChieYag]. If alignment layer is sufficiently conductive, after switching the applied field to zero, charge flows to balance the interface charge, which eliminates the depolarization field.

The other mechanism of the bistability is related to the anchoring of the FLC molecules with substrates. In this approach, in thin cells, the anchoring energy of FLC's with substrates begins to play a decisive role. From the diagram of the FLC states [ClarkHa] follows that the sufficiently large cell thickness d and polar anchoring energies W_p do not promote bistability, because the helical and twisted states become more favorable. The existence of the field threshold above which the bistable states appear is

$$E_{th} = \frac{\sqrt{W_d}}{K}, \qquad 1.20$$

where K is the average elastic (Frank) constant, and W_d is non-polar part of the anchoring energy. In the work [NakaIch], it was demonstrated that the large values of the polar anchoring energy result in decreasing the optical stability. The

magnitude of the non-polar anchoring energy for large enough switching fields does not affect the bistable behavior [NakaIch]. However, the case of the high polar anchoring energy leads to the disappearance of the bistability or, in other words to monostability.

1.2.4 Thresholdless hysteresis- free electrooptical mode (V-shaped switching)

During the last years, research on chiral smectic liquid crystals has been largely devoted to understand the origin of the analog thresholdless “V-shaped” switching mode, which was observed for the first time in some homologues of the antiferroelectric LC by S. Inui *et al* [Inui].

For the experimental observation of this mode, the FLC cell should be oriented in such a way that the transmission axis of the entrance polarizer is perpendicular to the layers normal (see Fig. 1.7) and the driving electrical voltage should have a triangular form.

The name of the “V-shaped” arises from the form of the electrooptical response resembling the Latin letter “V” (see Fig. 1.8). However, in contrast, the typical electrooptical response of the ferroelectric liquid crystals has, in this experimental geometry, resembles the letter “W”, which means existence of the threshold and the hysteresis.

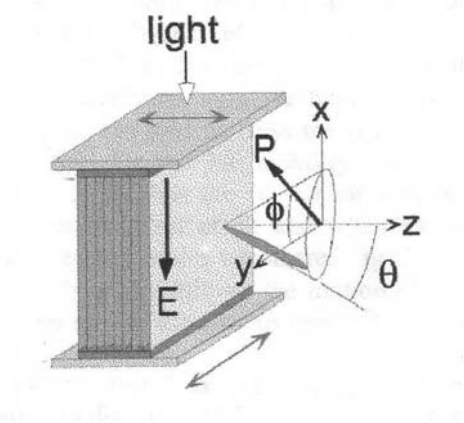

Figure 1.7: The arrangement of the polarizers and a FLC cell for observation of the V-shaped mode

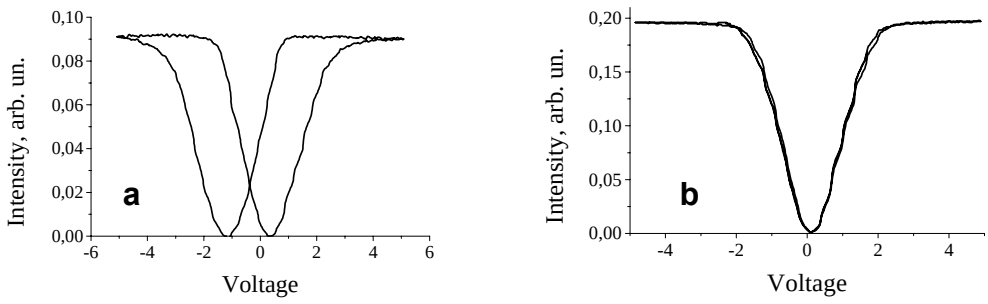

Figure 1.8: a) W-shaped switching curve; b) V-shaped switching curve

2.1 Definitions

Here we will introduce the parameters describing the V-shaped mode.

Voltage coercivity

This is one of the most important parameters characterizing the V-shaped switching. It shows (see Fig.1.9) how strong the hysteresis is, and it is equal to half of the voltage difference (ΔU_C) between two states where the intensity of transmitted light is minimal.

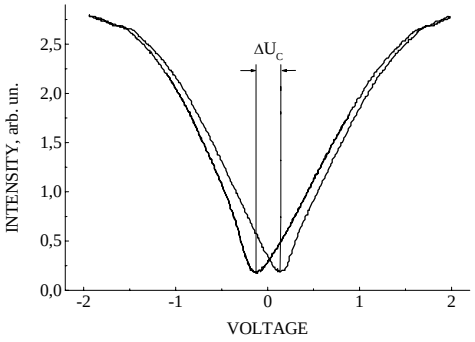

Figure 1.9: Definition of voltage coercivity

Saturation voltage

This is the value of the applied voltage above which, the transmission of the cell remains constant (see Fig.1.10).

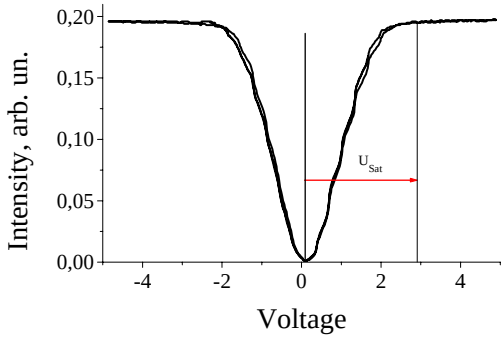

Figure 1.10: Definition of the saturation voltage

Inversion frequency

Inversion frequency f_i is the frequency of the driving voltage at which the hysteresis loop of the electrooptical response changes its direction from normal to abnormal (see Fig. 1.11). This frequency corresponds to the thresholdless switching.

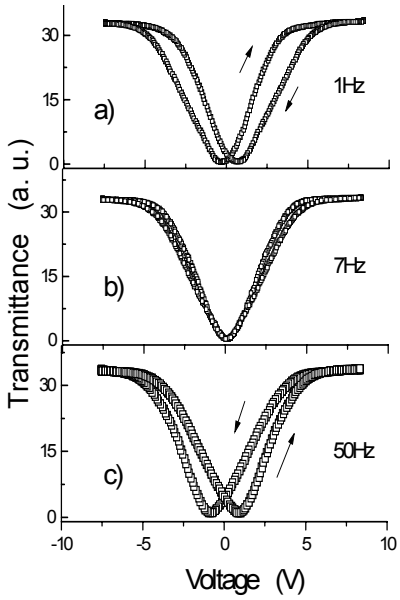

Figure 1.11: The inversion frequency f_i
a)normal hysteresis, b) V-shaped switching (inversion frequency),
c) inverse hysteresis

Approaches to explain the thresholdless switching mode

Random switching model of V-shaped switching

The first attempt to explain the nature of this effect was done by A. Fukuda and S. Inui [Inui, Fukuda]. This switching was first speculated to occur in a phase with randomly oriented C directors due to the reduction of the interlayer tilting correlation. The tilting correlation of the local in-plane directors between adjacent layers was considered to be lost because of the frustration between ferroelectricity and antiferroelectricity. It was confirmed that the substrate interfaces destroy the antiferroelectric order in thin homogeneous cells, apparently promoting the randomization of the local in-plane directors from layer to layer. The dynamic switching behavior were explained by the random model based on the two dimensional Langevin function [Inui, Fukuda, FukudIsh] under strong influence of an electric field and surface conditions [SeoNish, SeoGao, SeoTak, SeoIsh, Chand]. Nonlinear optical studies showed strong optical second harmonic generation signals at normal incidence from V-shaped switching cells [SeoPar]. This result seemed to be also explained by the two-dimensional Langevin potential, supporting the random model. Later, however, it was demonstrated that a switching model of the other extreme against the random model, i.e. the highly coherent azimuthal angle rotation model (collective model) is much more appropriate to interpret the V-shaped switching than the random model [ParTak].

Collective molecular motion model of V-shaped switching

The next model which was propose for explanation of the V-shaped nature is, so called, the collective molecular motion model. In this model, it is considered that reorientation of the FLC's goes in other, collective way. It means that the molecules along the cone collectively switch. The origin of such behavior was explained by competition of ferroelectric and antiferroelectric interactions [SeoIsh, GorMie]. Because such frustrated system is very soft and the relaxation time becomes long, molecules change their steady state orientation continuously

under the surface constraint and varying field, resulting in the collective motion. The collective motion was confirmed by the investigation of the second harmonic generation (SHG) and SHG interferometry [ParNak]. In this work, the second harmonic was observed in a homogeneously aligned SmC* cell at normal incidence. The SHG profile were detected as a function of applied electric field for four combinations of input-output polarizations of light of a YAG:Nd laser. It was supposed that the FLC had C_2 symmetry. Comparison of the theoretical and experimental results showed that the collective model adequately describe the behavior of the SHG. By using SHG interferometry measurements, it was found that the azimuthal rotation of the FLC molecules is limited within the half of the cone, where molecules could distribute. Moreover, it was also found that the FLC molecules undergoes counterazimuthal rotation in the upper and lower halves of the FLC layer in the chevron structure. The stabilization of the uniform molecular alignment was attributed to the escape from the formation of polarization charges and surface molecular constraint.

The other confirmation of the collective motion model was demonstrated in [ParTak].

Here the molecular motion of the FLC molecules were comprehensively investigated by measuring the effective optical anisotropy, apparent tilt angles, switching current and SHG. The same parameters were theoretically simulated based on two extreme models: collective model and random model. From these results, it was demonstrated that the FLC molecules do not switch randomly but rotate collectively on a cone under the driving field.

In the work [Hayashi], molecular orientation order parameters have been studied by Raman scattering in two types of LC materials showing V-shaped switching and having antiferroelectric phase. The results showed two extreme distributions of the local in-plane director at the tip of the V-shaped switching. One of compounds exhibited a small distribution, while the other exhibited a large distribution. The small distribution of the local in-plane directors suggests the collective azimuthal angle rotation in the V-shaped switching. However, the same explanation does not hold for the sample with large distribution. It was demonstrated that the essential for V-shaped switching is easy the formation of

invisible microdomains. This requires softness with respect to the tilting directions which follows from the frustration between ferro and antiferroelectrisity. The difference in the distributions for these two mixtures at the tip of V was explained by the barrier between synclinic and anticlinic ordering in adjacent layers. The small barrier gave a large distribution in the dynamic switching, consequently triggered the V-shaped switching and the large barrier did a small distribution and the tristable switching.

Despite all described studies and confirmations of the collective motion model, the nature and driving forces of the V-shaped switching is nevertheless unclear. The authors of [ParTak, ParNak] tried to explain the nature of V-shaped switching by the effect of the polarization charges. They speculated that the softening of the system might influence the effect of the polarization charge through an elastic constant. In the same time, it was not experimentally demonstrated that the mixtures showing V-shaped switching are really soft. In the work [Shiba], authors reported the temperature and frequency dependencies of the layer compression modulus B of a liquid crystal mixture showing V-shaped switching, where they observed a softening of the smectic phase in a SmX* phase. It was supposed that the softening could be attributed to the disorder of the layer structure. Moreover, it was also found that B in the soft smectic phase has a characteristic frequency dependence which is relevant to the relaxation time. The softening of the system, and particularly the relaxation phenomenon due to the external forces, has a strong influence on the polarization charge effect.

Electrostatic model of V-shaped switching

According to the “block model“ proposed by Rudquist *et al* [ClarBar] any conventional FLC with high self-interacting spontaneous polarization automatically forms a block of uniformly oriented local P_s. Under external field the whole block is switched and the kinks play a role of a surface lubricant for the director reorientation. The dielectric layers are supposed to play a crucial role keeping charges necessary to stabilize such a block-kink structure. Very high P_s and screening the field in the liquid crystal layer are necessary in this model. It

was especially stressed that the switching of polarization is thresholdless due to formation of the “blocks” mentioned above [RudWa].

In the work of N.Clark *et al* [ClarCol], electrostatic model of the thresholdless hysteresis free switching was further developed. In the first approximation, they supposed that free ions were absent inside this sample. In the initial stage of the switching process, the voltage drop V is equal to zero. The anchoring of the FLC at alignment layers is planar. As a result, the minimum surface energy exists in that case when the vector of the spontaneous polarization P_s is perpendicular to the surface. However, the anchoring energy of P_s is different for two cases, namely, for P_s pointing out or into the surface. Therefore, the surface anchoring energy can be decomposed into a nonpolar (independent on the sign of P_s) W_{np} and polar W_p parts The nonpolar energy is responsible for the bistability. The x-component of the P_s induces the surface polarization charge which must be compensated by free charges on the electrodes. The electrodes are separated from the FLC by the alignment layer. As a consequence, an electric field is created in the alignment layer. When the electrostatic energy of this field exceeds the nonpolar part of the anchoring energy, it is energetically favorable for the surface anchoring to break, so that the P_s becomes parallel to the cell substrates. As result, the cell becomes monostable.

The polar part of the anchoring energy forces P_s to be splayed in both monostable and bistable states, and polarization charges in this state gives contribution to the electrostatic energy.

The electrostatic energy of the alignment layers is proportional to the square of P_s. The non-polar contribution to the anchoring energy is independent of P_s. Hence, the monostable state is obtained for materials with high Ps. When an external voltage is applied to the monostable cell, P_s turns by an angle ϕ, so that the total electric field in the FLC layer is equal to zero. The voltage across the cell is due to an electric field induced in the alignment layers by P_s. It leads to a relation between V and ϕ:

$$V = \frac{2dP_s \sin\phi}{\varepsilon_1 \varepsilon_0}.$$

Here d and ε_1 are the thickness and dielectric constant of the alignment layer. When $V > V_c = \frac{2dP_s}{\varepsilon_1\varepsilon_0}$, the spontaneous polarization is aligned perpendicular to the cell substrates and can not compensate the external field so that the total field inside the FLC is not zero. The direction of the optical axis is directly related to ϕ, and the cell placed between two crossed polarizers demonstrates V-shaped switching.

The important question of the dynamic behavior of the V-shaped cells in the electrostatic model was investigated by M. O´Callaghan [Ocal]. He deduced relation between the FLC response time for bistable switching τ_{SSFLC} and the V-shaped response time τ_0:

$$\tau_0 = \frac{V}{V_S}\tau_{SSFLC} \quad . \qquad 1.31$$

$$V_S = \frac{2dP_S}{\varepsilon_1}$$

As one can clearly see, the response time of the V-shaped switching cells are slower than that of cells with bistable switching. The reason for such behavior is very simple: the bistable cells are driven by the higher voltage in comparison with V_S.

Up to now, we discussed the dynamics of the V-shaped switching cell behavior in the most simple approximation of the electrostatic approach, namely, by neglecting the influence of the surface forces. In the same work [Ocal], the influence of the surface anchoring on the dynamics of the V-shaped switching mode was taken into account. O'Callaghan demonstrated that due to the anchoring energy, the response time did not diverge to infinity as it happens in the pure electrostatic approach.

In work of M. Čopic, *et. al* [Cop], authors extended their electrostatic approach to the case of the presence of ions in the FLC. In this new situation, the external electric field applied to the FLC layer will result in a spatially inhomogeneous distribution of ions which partly screens the applied field. The ions, during the switching process, drift and diffuse from one substrate to another. This ions

movement creates an additional inhomogeneous electric field. Because the total field is zero, the electric field due to reorientation of the spontaneous polarization is also inhomogeneous. The result of this effect is the following: The optical axis of the FLC is oriented differently throughout the cell and the optical response is asymmetric around the extinction points. The ionic contribution to the field opposes the external field, the polarization field crosses zero before V=0, so that by going from the negative voltage peak the optical extinction also occurs for some small negative value of V. As the result, one can obtain an inverse hysteresis.

The polar anchoring model

S. Elston and N.J. Mottram [Elst1, Elst2] proposed that the polar anchoring, which induces ferroelectric ordering close to the cell surfaces, in a cell containing antiferroelectric liquid crystals are responsible for existence of the V-shaped switching mode. Their model includes effects due to finite polar and nonpolar anchoring, quadrupolar ordering and polarization self-interaction. By minimizing the free energy of the system, they found parameters domains where multiple zero-voltage solutions were stable. They also found that these solutions might undergo thresholdless or hysteresis switching depending on the parameter values.

Summary

As we can see there are different approaches to explain the nature of the thresholdless switching. But in the same time, they are very contradictive.

For instance, the collective motion model requires the existence of the special mesophase SmX*. In the same time, it is well known that the V-shaped switching exists also in usual FLC's.

The electrostatic model claims that for this electrooptical mode high spontaneous polarization is necessary. But it is known that the V-shaped switching can be observed in mixtures with the low value of the spontaneous polarization

The polar anchoring model is based on the assumption that the V-shaped switching exists only in a special geometry with strong polar anchoring of the antiferrolectric liquid crystals with the cell substrates. However, experiments show

that the thresholdless switching can be observed in usual cells without special treatment filled with ferroelectric liquid crystals.

In addition, authors of the electrostatic approach and the polar anchoring model did not demonstrated any experimental evidence of their theories.

However, several important facts concerning the V-shaped mode were found.

First of all, the importance of the alignment layer was experimentally and theoretically demonstrated. Then the importance of the electric field applied to the FLC layers were revealed.

These results were a hint for us during the developing the Dynamic Voltage Divider model, which can describe and predict this unusual electrooptic behavior of FLC's [Blm1, Blm2]

Chapter №2

Experimental part

In this chapter, we will describe the experimental techniques applied for the observation of the V-shaped switching, measuring the basic parameters of the FLC's, cells preparation technology, FLC materials chosen for our investigations as well as the software developed for modeling the FLC cells.

2.1 Experimental Setup

For characterization of the cells and investigation of the electrooptic behavior of the V-shaped switching mode, a special setup was utilized (see Fig. 2.1). This setup consists of several parts which can measure simultaneously several

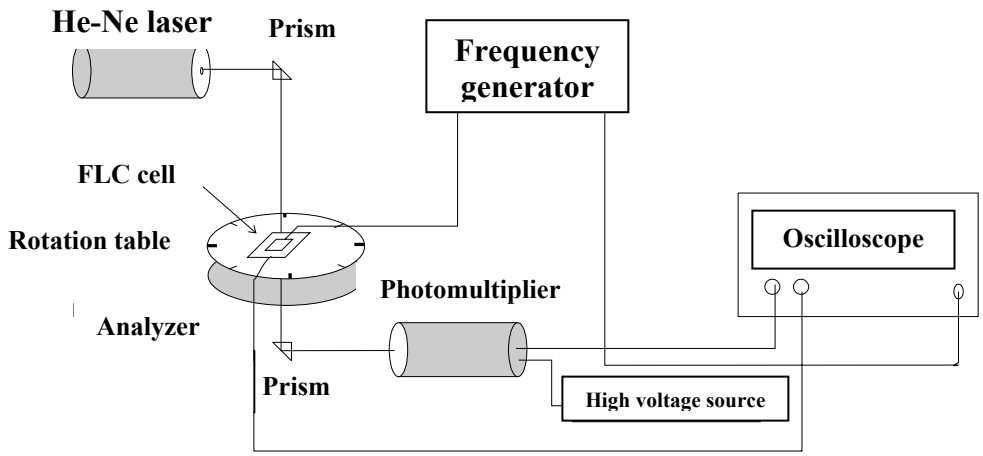

Figure 2.1: Experimental setup for investigation of FLC cells

parameters of the cell. The source of the light is a He-Ne laser with wavelength $\lambda = 633$ nm and power P=5 mW. In order to remove other wavelengths (appearing due to plasma discharge) from the light spectrum, a filter centered at $\lambda = 633$ nm and a linear dichroic polarizer were installed in front of the laser. The linearly polarized laser beam is deviated by the right-angle prism into the sample, which is mounted inside the temperature-stabilized chamber. The temperature is controlled and stabilized by the Eurotherm temperature controller.

The accuracy of the temperature stabilization is about 0.1° C. In the same time, the temperature chamber is mounted on a rotation table which is controlled by the Newport motion controller with accuracy 0.05°. The liquid crystal cells are driven by the programmable frequency generator "HP 33120A". The modulated light is

directed by the second prism into a photomultipler (PM) through the linear polarizer crossed with respect to the input one. The PM is driven by a high voltage power supply unit. The signal from the PM is detected by a multichannel oscilloscope “HP Infinium”.

This setup also allows us to measure the current flowing through the FLC cell. For this purpose, the FLC cell is attached in series with a resistor from which the signal was recorded by the oscilloscope.

Measurement of the tilt angle

The measurement of the tilt angle of the FLCs can be carried out by the application of the square waveform voltage. In this case, the switching can be easily detected by the above-described setup. In order to do it, one should turn

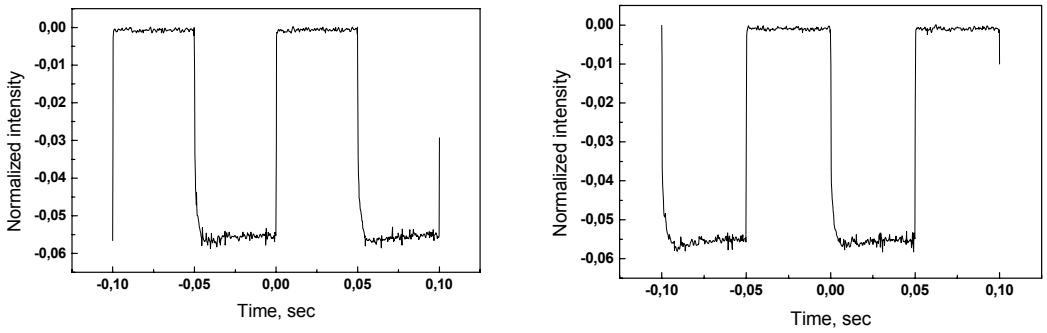

Figure 2.2 : Measurement of the tilt angle θ; typical form of electro-optical response at two extreme positions of the cone: a) angle θ; b) angle -θ.

the rotation table in such angular position that one of the extreme position of the cone (say θ) coincides with the transmission axis of the analyzer. The transmission of the light becomes equal to zero. By applying the electric field, the transmitted intensity increases (see Fig. 2.2 a). Then, if the cell is rotated to the opposite position (-θ) coinciding with a polarizer, the electrooptical response change its polarity (see Fig. 2.2 b). It means that the cell is turned at angle 2θ . The value of the tilt angle can be easily derived from it.

Measurement of the response time

For measurement of the response time, a rectangular waveform voltage with low frequency (usually 1-10 Hz) and strong enough to completely switch the FLC molecules should be applied to the cell. Then, FLC cell should be turned in such a position that one of the extreme positions of the cone coincides with the orientation of the polarizer or analyzer and the polarity of the electrooptical response is similar to that of the applied square wave.

The response time of the FLC is, according to the definition, the time difference between 10% of the transmitted intensity and 90 % of it (see Fig. 2.3).

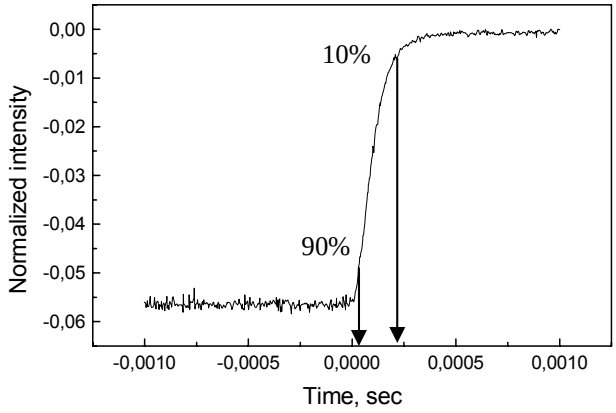

Figure 2.3: Measurement of the switching time: electrooptic response

Measurement of the spontaneous polarization and conductivity

The measurement of the spontaneous polarization is based on the investigation of the repolarization current flowing through the cell upon application of the low frequency triangular voltage (see Fig. 2.4). For that purpose, an additional resistor with low resistivity R (several kΩ) is placed in series with the oscilloscope. The voltage on this resistor transforms the current into the voltage. The characteristic peak on the oscillogram corresponds to the spontaneous polarization. To measure the P_s, one should measure the area of this peaks or, in practice, the number of the elementary cell (seeing in the oscilloscope) N inside this area. Then, knowing the resolution of these cells (Δt and ΔU) as well as the area of the FLC cells A, it is easy to calculate the spontaneous polarization:

$$P_s = \frac{N\Delta t \Delta U}{2RA}.$$

The FLC layer resistivity can be also measured from the repolarization current. To do it, one should measure the voltage drop *V* on the slope of the repolarization current (I_σ). The resistivity, after that, can be calculated as:

$$R_{FLC} = \frac{U_{ap}}{V} R,$$

where U_{ap} is the amplitude of the applied voltage.

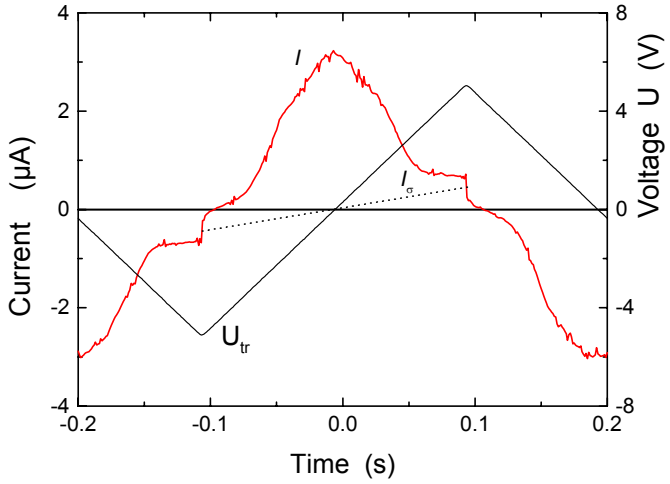

Figure 3.4: Measurements of the spontaneous polarization and the conductivity of FLC mixtures (I – repolarization current)

2.2 Materials

In experiments for investigation of the V-shaped switching, numerous FLC cells were utilized. However, all of them were of a sandwich type consisting of two glass plates covered by transparent conductive films of Indium-Tin-Oxide (ITO). On the top of the ITO electrodes, alignment polyimide layers of different thickness d_p were deposited by spin coating technique. Their thickness was measured by an AFM technique. As a rule, only one alignment layer was rubbed. The gap between the glass substrates was between 1 and 2 μm and installed with microscopic polymer microbeads dispersed along the perimeter of the electrode overlapping area. The thickness of the gap *d* was measured on the empty cells by a capacitance technique and afterwards the cell was filled with a liquid crystal in the isotropic phase.

All measurements were only carried out in the smectic C* phase of FLC's described in Table 1.

Name	Phase sequence	P_s (nC/cm^2)	Tilt angle Θ (deg)	Viscosity γ_φ (Pa.s)*	Pitch (μm)
FLC-422[1)]	Cr-10°C-SmC*-58°C-SmA-80°C-Iso	100	23.5	0.07	∞
CS-1025	Cr- -3°C-SmC*-62°C-SmA-84°C-N-90°C-Iso	16.4	21	0.04	10
FLC-36[1)]	Cr→3°C→SmC*→35°C→SmA→62°C→Iso	21	15	0.03	∞
PBH-13[2)]	Cr-20°C-SmC*-87°C-SmA-100°C-N-101°C-Iso	130	35	0.4	0.2
Felix 015/000	SmX -11°C-SmC*-71°C-SmA-83°C-N-86-83°C Iso	9-10	24	0.06	100
FLC-438[1)]	Cr-12°C-SmC*-82C* - SmA – 103°C – Iso	85	28	0.27	0.2

*Rotational viscosity defined as $\gamma_\varphi=\gamma_0\sin^2\Theta$

[1)] Lebedev Physical Institute, Moscow, Russia

[2)] Darmstadt University of Technology, Darmstadt, Germany

Table 1: FLC materials used in the present work (T=25°C)

A particular material and cell were chosen according to the idea of the experiment. The textures and phase transitions were studied under a polarizing microscope. The kinetics of the repolarization currents and of the optical response of the FLC to the triangular voltage form were investigated using the set-up described above.

Cell №	FLC mixture	Area, cm^2	Cell thickness, μm	Alignment/ Insulating layer thickness, nm
1	FLC 422	1.4	1.7	80
2	Chisso 1025	0.16	2	40
3	FLC 36	0.16	2	40
4	PBH 13	1.3	1.4	40

Table 2: Main FLC cells utilized in the present work

2.3 FLC cell fabrication

The liquid crystal cells are the key element of any device based on these materials. Therefore their quality plays a crucial role both for fundamental investigation and practical applications. Concerning to FLC cells, the requirements imposed to their quality is more severe than those for NLC cells. They are connected with the physical properties and applications of FLC's. Namely, the cell gap should be in the range 0.8 – 2 μm and , in the same time, its spatial homogeneity should be very high. The alignment layer should not have any volume or surface defects or spatial inhomogeneouty of the thickness. These requirements make the fabrication technique of the FLC cell much more complicated in comparison with NLC cells preparation. Some of the cells prepared are characterized in Table №2.

In this paragraph, the detailed technology of the FLC cell preparation will be presented.

FLC cell structure

A conventional FLC cell has rather simple structure. It consists of two glass substrates separated by a liquid crystal layer. The glass substrates are sputtered with the conductive ITO electrode. Sometimes, insulating layers like Al_2O_3 are deposited over the electrodes to prevent electrical breakdown or to control the capacitance of one of the arms of the voltage divider formed by this and FLC layers. To create an ordered FLC structure, each electrode is covered with polymeric alignment layer The cell gap is predetermined by spacers placed between the two substrates (see Fig. 2.5).

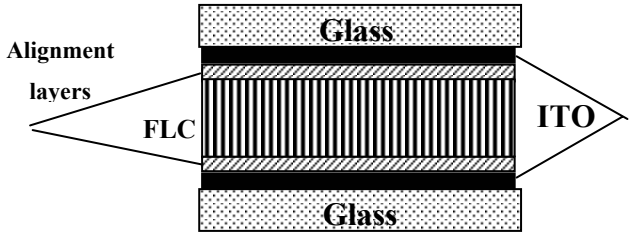

Figure 2.5: Structure of a FLC cell

Preparation of the alignment layers

One of the crucial things for the FLC cell is the quality of the alignment layers. In turn, it depends on both the clearness of the cell substrates and the materials chosen as alignment layer. The former one is possible to control during fabrication process, the latter one depends on a supplier.

Cleaning of the substrates

The glass substrates for the cells are usually cutted from the big sheets of the ITO coated glass. The dimensions of the substrates strongly depend on the forthcoming experiments. Usually it is 12x15 mm. Along the perimeter of each substrate a ITO-free strip with thickness 1÷1,5 mm is created either by lithographic techniques or by the mixture of Zn powder and 10% solution of HCl. These stripes will be necessary to disperse spacers along them

After that, substrates should be cleaned in several steps:

1. Washing them in ultrasonic bath filled with 50% solution of methanol during 15 minutes to remove the Zn powder particles.
2. Washing in a high purified chromosulfuric acid during 10÷20 seconds to clean the substrates from strong organic contamination.
3. Washing in distilled water during 2÷3 min. to remove chromosulfuric acid.
4. Washing in high purified 30% solution of H_2O_2 during 30 minutes to remove remaining organic contamination.
5. Washing in distilled water during 10 minutes to remove H_2O_2.
6. Washing in highly purified 90% ethanol to remove water and "dry" the substrates
7. Final cleaning of the substrates in a plasma cleaner to remove molecular carbon compounds by plasma discharge in the air or argon atmosphere during 20-30 minutes.
8. The spin-coating device switched off, then a droplet of polymer solution is placed just in the middle of the ITO layer. This droplet has to cover simultaneously all ITO surfaces. This is a second criterion of the process validity. If the situation described above does not work, it means the polymer or is not pure enough.

After that the substrates are ready for spin coating of the polymer (usually polyimide) alignment layers.

Spin coating of the alignment layers

The thickness and uniformity of the alignment layers depend on both the rotation speed of the spin-coating device as well as the concentration of the polymer. It is very difficult to give any recipe in advance. Nevertheless, the spin-coater rotation speed with about 3000 revolutions/min gives the polymer layer thickness for our material of around 30nm depending on temperature and ITO layer quality. The rough criterion that polyimide is more or less homogeneously covered over the substrate is the absence of the interfereometric fringes in light reflected from the substrate.

The polymer layer thickness was controlled by the AFM (Atomic Force Microscope) operating in the contact mode.

The baking of the alignment layers is implemented in two stages.

The first stage is heating them from room temperature to 120^{o}C during 1 hour and further prebaking at this temperature during one hour.

The second stage is baking the substrates at the temperature of 180 -190^{o}C during three hours.

The final stage of the substrates preparation is the rubbing of polymer layers by a special rubbing machine (10 cycles, 95 rpm, 20 cm/min).

After that, the electrical contact is attached to the substrate as it is shown in figure 2.6. In order to do it, a special glue BF-2 can be used. A narrow border stripe of ITO (about 1 mm) was covered by a solution of BF-2 in ethanol, and then a cable was fixed by ordinary soldering iron. Low temperature soldering alloy can also be used for this purpose.

Spacers distribution over the substrates

We used calibrated polymer microbeads as spacers. The spacers may be distributed on surfaces in different ways. However, in this work, spacers dissolved in *iso*-propanol were distributed along the ITO-free area of the glass substrates (see Fig. 2.6).

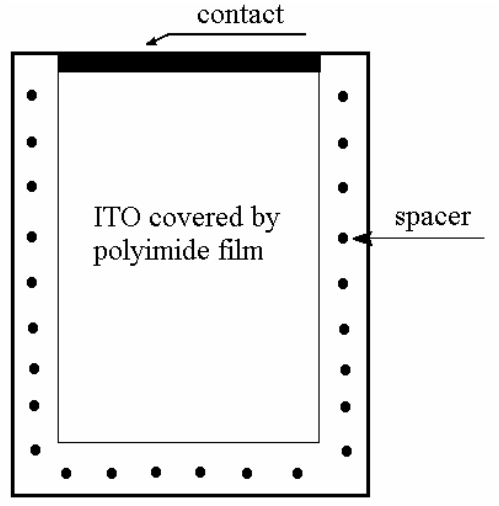

Figure 2.6: ITO covered glass with spacers and electrical contact.

Assembling the FLC cells

To assemble a cell, two substrates, one with the spacers and the other without them are placed one over the another and fixed in a special mechanical device (holder), which allows the variation of the mechanical pressure in several points of a cell. The active area of the empty cell is visible for an operator. It allows to estimate uniformity of the cell gap visually by observation of the optical interference fringes. The operator can reach the uniformity of the cell gap by applying variable mechanical pressure in several points (at least 4 points) by using micrometric screws. The thickness of the empty cell is estimated either by measuring its capacitance or by investigation of the transmission spectra.

Then the empty cell, fixed in this mechanical holder, is heated up to 120^{o}C and cooled down to room temperature. The cell gap uniformity must be independent on this process in order to avoid any deformation of the FLC layer, because they give rise to the defects, which are hardly removable. It is a general disadvantage of all FLC's known as a "shock problem".

The filling of the cell with FLC material is made from its isotropic phase, at the temperatures 100÷130^{o}C in a vacuum chamber to prevent the appearance of the air bubbles. If bubbles appear they create the defects of the FLC texture

At the final stage, a cell has to be glued by an epoxy glue along its perimeters.

2.4 Computer simulation of FLC cells

The software for computer modeling of the electrooptic effects in FLC's was developed by Dr. S.S. Palto (Institute of Crystallography, Russian Academy of Sciences, Moscow). The detailed description of this package was published in [Palto1].

This software includes the following equations and assumptions:

Basic principles

A surface stabilized FLC cell with substrates in the *xy* plane was considered. The smectic layers with a normal $\boldsymbol{k}=(k_x, k_y, k_z)$ to them form an arbitrary angle with the *xy* plane, the molecules are tilted at the angle Θ with respect to smectic normal $\boldsymbol{k}$. A FLC is anchored at the opposite boundaries at arbitrary angles and both the zenithal and azimuthal anchoring energy may be varied. It is essential that the alignment layers have finite capacitance and conductivity. The permanent conductivity of a FLC is also taken into account. A voltage of an arbitrary form may be applied to transparent electrodes. Note, that the voltage across the liquid crystal layer is not fixed, its magnitude and form depend on the permanent impedance of the two aligning layers and dynamic (voltage and time dependent) impedance of the FLC layer. This makes a solution of the problem much more difficult. The Lagrange-Euler equations for the FLC bulk in the absence of flow were considered. They include the elastic, electric and viscous torques.

Elastic energy and elastic torques.

The elastic energy is taken in the form (see eq. 1):

$$F_1 = \frac{1}{2}\left[K_{11}(div\,\mathbf{n})^2 + K_{22}(\mathbf{n}\bullet rot\mathbf{n} + q_0)^2 + K_{33}(\mathbf{n}\times rot\,\mathbf{n} - \mathbf{b})^2 + K_4\left(\cos\Theta - \mathbf{n}\bullet\mathbf{k}\right)^2\right], \quad (1)$$

where K_{ii} are Frank moduli (K_{11} - for the bend deformation, K_{22} – for the splay deformation, K_{33} – for the twist deformation) and K_4 describes compressibility of smectic layers related to a change in the tilt angle Θ, q_0 and **b** describe spontaneous twist and bend of the director **n**. The coefficient K_4 is defined from a virtual work that is necessary to change the layer thickness by amount $\delta\sim(\cos\Theta$ -

$\cos\vartheta$) without penetration of molecules from one smectic layer to another. Its physical sense becomes clear if we consider a work $\delta A \cong a(\vartheta-\Theta)^2/2$ for a small deviation of the tilt angle ϑ from its equilibrium value Θ, like in the Landau expansion near the A-C* transition, where $F \approx (1/2)a\vartheta^2+(1/4)b\vartheta^4$. Then $K_4 = a/\sin^2\vartheta$ and its finite value allows modeling the electroclinic effect at any temperature. Assuming a uniform director distribution in the *xy* plane, we obtain three components of the elastic torque.

Electric energy and electric torques.

If the charge (not voltage) is fixed at the boundaries of a FLC, the electric contribution to the free energy density is positive $F_2 = \mathbf{D}_i\mathbf{E}/2$. Here $\mathbf{D}_i$ describes a field induced contribution to the total displacement $\mathbf{D} = \mathbf{D}_0 + \mathbf{D}_i \equiv \mathbf{P}_s + \boldsymbol{\varepsilon}\mathbf{E}$, $\boldsymbol{\varepsilon}$ is the dielectric permittivity tensor which defines the anisotropy $\Delta\varepsilon = \varepsilon_{//} - \varepsilon_\perp$, $\mathbf{D}_0 = \mathbf{P}_s$ is the spontaneous polarization. For $\mathbf{E}=(0, 0, E_z)$, and $\mathbf{D}_i = (D_{xi}, D_{yi}, D_{zi})$ we obtain

$$F_2 = \frac{D_{zi}E_z}{2} = \frac{(D_z - P_{sz})^2}{2\varepsilon_\perp\left(1+\frac{\Delta\varepsilon}{\varepsilon_\perp}n_z^2\right)}. \qquad (2)$$

Due to chiral symmetry of the SmC* phase $P_{sz} = P_0\left[(\mathbf{k}\bullet\mathbf{n})(\mathbf{k}\times\mathbf{n})\right]_z$, where P_0 is the tilt-polarization coupling coefficient $P_0 = P_s/\left[(\mathbf{k}\bullet\mathbf{n}_0)(\mathbf{k}\times\mathbf{n}_0)\right] = P_s/\cos\Theta\sin\Theta$.

Substituting this into (eq. 2) and differentiating the latter we obtain all the three components of the electric torque exerted on the director as well as the total D_z and field induced D_{zi} displacement .

Anchoring energy and boundary conditions

The anchoring energy is taken in the Rapini form:

$$W = W_{x'} + W_{z'} = (1/2)(W_a n_{x'}^2 + W_z n_{z'}^2),$$

where W_a, W_z are amplitudes of the azimuthal and zenithal components of the energy in the local coordinate system with the *y′* axis corresponding to the easy direction and *z′* axis is in the *y′z* plane. In the laboratory *xyz* system the easy axis

is defined by angles φ_a, θ_a with respect to the *x* and *z* axes, correspondingly, and the expression for the anchoring energy reads (eq. 3):

$$W = \frac{1}{2}W_a(n_x \sin\varphi_a - n_y \cos\varphi_a)^2 + \frac{1}{2}W_z(n_z \sin\theta_a - n_x \cos\varphi_a \cos\theta_a - n_y \sin\varphi_a \cos\theta_a)^2 \quad (3)$$

Viscous torque

As the mass transfer is disregarded, we consider only the second rank rotational viscosity tensor. In the local system corresponding to the SmC* symmetry the tensor $\boldsymbol{\gamma}_L$ has three different principal components γ_1 ,γ_2 and γ_3. The component γ_2 corresponds to the director rotation along the conical surface and is related to the conventional value $\gamma_\varphi/\sin^2\Theta$, and both $\gamma_1 \cong \gamma_3 \cong \gamma_\theta$ correspond to a change in the director tilt. After applying the similarity transformation $\boldsymbol{\gamma} = \mathbf{R}\boldsymbol{\gamma}_L\mathbf{R}^{-1}$, where **R** is the rotation matrix, we find the viscosity tensor in the laboratory frame and the corresponding viscous torque.

Full set of equations including the elements of the electric circuit

Two FLC aligning layers can be considered as one capacitor *C* and resistor *R* connected in parallel. The resistance of electrodes R_0 is also taken into account in series with the output resistance of the voltage source. For the current and voltages in the circuit (eq.4):

$$\frac{dU_C}{dt} + \frac{1}{C}\left(\frac{1}{R} + \frac{1}{R_0}\right)U_C = \frac{1}{CR_0}(U - U_{LC}), \qquad \frac{U_{LC}}{R_{LC}} + S\frac{dD_z}{dt} = I, \qquad U_{LC} = U - IR_0 - U_C \quad (4)$$

Here *S* is the electrode overlapping area; *U* , U_C and U_{LC} are voltages across the electrodes, orienting layers and the FLC; *I* is the current from the source; D_z is the *z*-component of the electric displacement in a FLC with the constant Ohmic resistance R_{LC}.

The set of equations (4) together with the general vector-form expression for the balance of elastic, electric and viscous torques

$$\boldsymbol{\gamma}\dot{\mathbf{n}} = -\frac{\partial F}{\partial \mathbf{n}} + \frac{d}{dz}\frac{\partial F}{\partial \mathbf{n}'} + \lambda\mathbf{n}, \quad F = F_1 + F_2, \qquad (5)$$

where λ is the Lagrange multiplier, and the boundary conditions (e.q 3) presents the full set of equations which allows the calculations of time and spatial dependencies of the director distribution in terms of the azimuthal φ (U,z,t) and polar ϑ (U,z,t) angles at any voltage. With these functions, we are able to calculate a current in the circuit I (U,t), and a voltage across the FLC layer U_{LC}(U,t). Then, using the Berreman matrix method and a new algorithm described in [Palto], the optical transmission of the cell T(U,t) is calculated with properties of other optical elements (a light source, polarizers, conductive glasses, aligning layers, etc.) taken into account.

Chapter №3

Experimental investigation and computer modeling of the thresholdless switching in Ferroelectric Liquid Crystals

In this chapter, the nature of the thresholdless hysteresis free mode of FLC (V-shaped switching) will be investigated.

The theoretical background of the present work is the Dynamic Voltage Divider Model developed by W. Haase, S. Pikin *et al* [Blm2]. This theory is based on the assumption that the characteristic times of the FLC cell (the field switching time of the director, the space charge relaxation time, the free relaxation time of the director) and the driving voltage should coincide. This theory gives some important predictions about behavior of the basic parameters of the V-shaped mode. The important consequence of this approach is that the thresholdless switching occurs only when the frequency and amplitude of the external voltage have unique values at given parameters of an FLC and alignment layers (or external circuit elements).

It will be demonstrated that the voltage divider formed by the FLC cell elements, such as alignment / insulating layers and FLC layer are crucial for the V-shaped switching mode. The influence of the characteristics of these elements (capacitance, FLC conductivity, spontaneous polarization, FLC texture quality) on the performance of V-shaped mode will be demonstrated. The experimental data will be compared with their computer modeling. In this connection, I would like to acknowledge advices of Prof. L. M. Blinov with whom we made this modeling and Dr. S. P. Palto who developed the FLC modeling software.

3.1 Electrical circuit of a FLC cell. Dynamic Voltage Divider

.A conventional FLC cell has rather simple structure. It consists of two glass substrates separated by a liquid crystal layer (see previous chapter). The glass substrates are sputtered with the ITO electrode. To create an ordered liquid crystalline structure, each electrode is covered with polymeric alignment layer. It is evident, that structure described above is electrically equivalent to a scheme shown in figure 3.1.

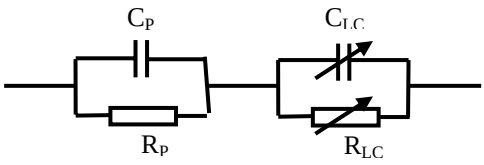

Figure 3.1 : Electrical circuit of a FLC cell (C_p and R_p are capacitance and resistivity of the alignment layers, C_{LC} and R_{LC} are capacitance and resistivity of the FLC layer, respectively

However, due to electrically induced reorientation of liquid crystal molecules (which is a dielectric media) and, hence, change of the effective dielectric constant, the capacitance of the cell is a function of the applied voltage. In other words, capacitance of the filled cell is a variable but not a constant value. At the same time, the resistivity of the liquid crystal layer is also function of the external parameters, such as, temperature and the external electric field. Really, the low-frequency dielectric constant of a FLC is typically about ε=100 and, with increasing field, decreases dramatically down to about ε=5 due to suppression of the Goldstone mode. Hence, the FLC layer capacitance C_{LC} changes with voltage (for 2 μm thick cell filled with Felix 015/000) from about 900 nF to 200 nF (see Fig. 3.2).

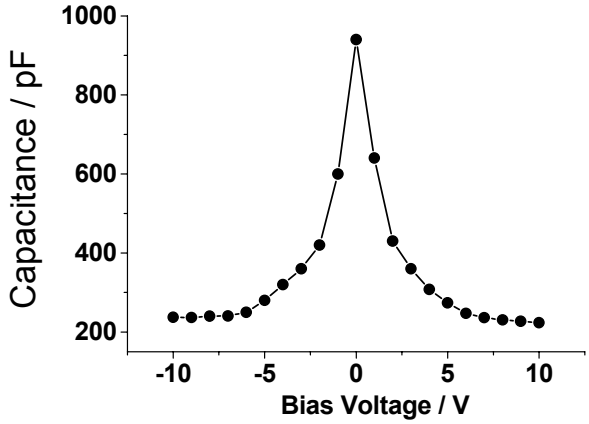

Figure 3.2: Dependence of the capacitance on the applied voltage, FLC mixture – Felix 015/000 (P_S=9 nC/cm^2, θ=22.5^0 at room temperature), cell thickness 1.76 μm, area of the cell 0.16 cm^2, the amplitude of the probe voltage and frequency are 0.1 V and 10 Hz, respectively, thickness of the alignment layers 30 nm;

The typical value of the specific resistance of the FLC's is $\rho \approx 10^{11}$ Ωcm at room temperature. Therefore, the *RC* time constant of the FLC's changes during their reorientation from 2 s to 100 ms.

At frequencies $f << (2\pi R_{LC} C_{LC})^{-1} \approx 10$ Hz the a.c. voltage on a FLC layer U_{LC} =B/(A+B) is controlled by two impedances, that of the polymer $A=(\omega C_p)^{-1}$ and that of a FLC layer $B=[(R_{LC})^{-1} + \omega C_{LC}]^{-1}$, the former is only frequency dependent, the latter dramatically changes with both the voltage and frequency (note, with increasing frequency, switching of spontaneous polarization is accompanied by

dielectric losses which also contribute to the R_{LC} value,). It is also of principal importance that both the parameters, determining the FLC impedance, especially R_{LC}, are strongly temperature dependent

It is easy to conclude from this discussion that the liquid crystal layer is electrically equivalent to the variable capacitance and resistivity connected in parallel. In addition, as was said, the thin polymeric film utilized as an alignment layer also has its own capacitance and very high resistivity.

Usually, one can neglect the resistivity of this layer. From the other side, the capacitance of the alignment layer is very important and its role in the V-shape switching as it follows from the Dynamic Voltage Divider model will be demonstrated in paragraph 3.1.1. A typical cell with V-shape response contains two thick polymer aligning layers, each about 50 nm thick and a 2 μm thick FLC layer. With cell area of 1 cm^2, dielectric constant of a polymer ε_p=2.6 and specific resistance $\rho_p \approx 10^{14}$ Ωcm, the polymer layer capacitance and resistance are about Cp≈50nF and R_p≈10MΩ, the characteristic RC time constant is τ_p≈500s. If one is not interested in frequencies $f << (2\pi\tau_p)^{-1} \approx 1$ mHz , the polymer resistance might be ignored and the circuit becomes simpler, see figure.3.3.

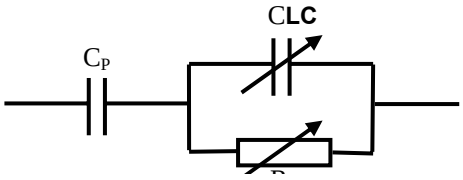

Figure 3.3 : Equivalent electrical circuit of the ferroelectric liquid crystal cell; C_p – capacitance of the alignment layer, C_{LC} – capacitance of the FLC layer, R_{LC} – resistivity of the alignment layer

Variable impedance of the FLC layer in conjunction with the capacitance of the alignment layer will result in rather interesting phenomena: the applied voltage, which has triangular form in our case, can be expanded in Fourier series. Then, due to these reasons, different components of this expansion will have a different phase. The amplitude of the voltage dropped on the FLC layer will be different in comparison with the applied one.

To conclude, the FLC cell is a typical voltage divider. As a result, some part of the applied voltage drops on the alignment layers but not on the FLC layer. In case, when a sinusoidal signal is applied, $U=U_0 \sin\omega t$, the voltage on the FLC layer can be written as

$$U_{LC} = -\frac{\omega R_{LC} C_p}{[1+\omega^2 R_{LC}^2 (C_p + C_{LC})^2]^{1/2}} U_0 \cos(\omega t + \delta) \qquad 2.1$$

$$\tan\delta = \omega R_{LC}(C_p + C_{LC}).$$

The characteristic time of the voltage divider is $\tau_d = R_{LC}(C_p + C_{LC})$ and, as we shall see further on, it is that time which mainly predetermines the hysteresis inversion frequency f_i.

The principal and quite general idea of the presented work is that the "thresholdless, hysteresis free" V-shape switching is rather an apparent, not real effect. The switching of the director of the liquid crystal layer, in reality, has a threshold and normal hysteresis if the optical transmittance is plotted as a function of the voltage on a FLC layer and not as a function of the total voltage on the FLC cell which always includes inner alignment/insulating layers.

3.1.1 Voltage divider with external electrical elements

In an FLC cell with the V-shaped response a polymer layer plays several roles: it aligns liquid crystal, forms a shoulder for the voltage divider and also is capable to discharge any surface charges accumulated at the liquid crystal-polymer interface. The Liquid crystal plays a role of a switcher and also contributes to a change in the dividing ratio. Therefore, to prove the unique role of the voltage divider, we can liberate the polymer from the second two functions and transfer them to external electric elements. The resistance of the liquid crystal can generally be controlled either by doping the material with ionic impurities or by temperature. However, we can also simulate these variations using external resistors parallel to the FLC resistance.

Figure 3.4 shows the same model cell as before but with additional C, R and R_1 elements. Two of them, C and R play the crucial role, as it is expected, they should increase the hysteresis inversion frequency. Resistor R_1 is optional, it provides a possibility to apply a d.c. bias voltage to the liquid crystal, or to discharge the liquid crystal cell (in case of some asymmetry) from electric charges accumulated on capacitance C_p or capacitor C.

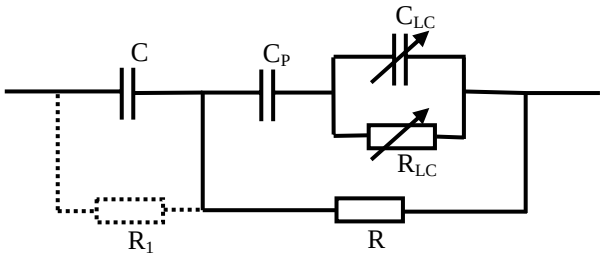

Figure 3.4: Equvalent electrical scheme of a FLC cell with an external resistivity (R) and a capacitor (C)

Now, it is possible to show how the hysteresis inversion frequency is easily changed by variation of external elements. First, we demonstrate a cell №1 (see table 2), which has an inversion frequency without external elements f_i =1.5 Hz at T=20°C. With external C and R elements, as shown in figure 2.8 but without R_1, the inversion frequency increases dramatically. The optical transmittance voltage forms are demonstrated in figure 3.5. With an additional capacitor C=22nF alone, the frequency is shifted from 1.5Hz to 8.9Hz. When resistors either R=180 or 82 kΩ are connected in parallel to the cell, the inversion frequency is further shifted up to 99Hz and 159Hz, respectively. The total shift of f_i is 106 times and the role of the RC constant is evident. The frequency dependence of the threshold (coercive) voltage on the cell alone and on the same cell in combination with C=22 nF and R= 180 kΩ is displayed in figure 3.6 (curves 1 and 2, respectively).

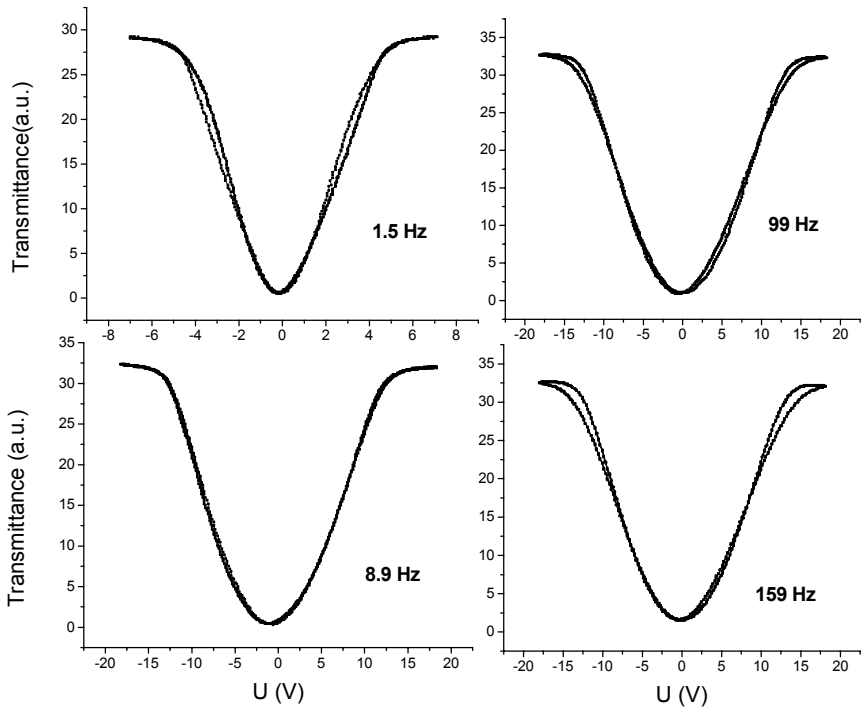

Figure 3.5: V-shaped optical transmittance of cell №1 in different regimes: a) without external elements, f_i = 1.5 Hz; b) with external capacitor C= 22nF, f_i = 8.9 Hz; ; c) with external capacitor C= 22nF and external resistor R=180kΩ, f_i = 99 Hz; d) with external capacitor C= 22nF and external resistor R=82kΩ, f_i = 159 Hz; temperature 20°C

The second example is, probably, even more demonstrative. The Cell №2 is a standard 2 μm EHC thick cell filled with the Chisso CS-1025 mixture having low value of spontaneous polarization (see tables 1 and 2). For such a cell no V-shaped switching is expected from any model discussed in literature. In fact, when the Chisso material is fresh, the hysteresis inversion frequency can be found at very low frequency, f_i =0.7 Hz. However, cell №2 was filled with aged, more conductive material (small R_{LC}) and, as expected from the above consideration, the V-shape switching is observed at a higher frequency 3.5Hz. With an external capacitor C=2.7nF the hysteresis inversion frequency increases 150 times and reaches 530Hz at room temperature (see Fig. 3.7). The frequency dependencies of the coercive field for both cases, with and without capacitor, are very similar to those shown in figure 3.6.

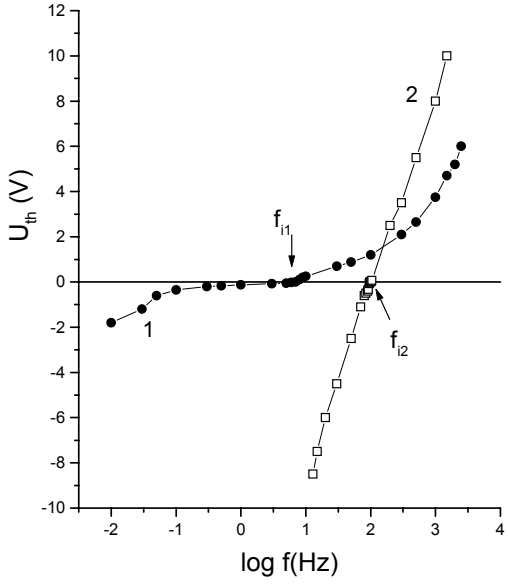

Figure 3.6: Threshold voltage for optical transmittance as a function of frequency for cell №1. 1) triangular voltage ±9V is applied directly to cell electrodes; 2) triangular voltage ±18V is applied to the cell through a capacitor C=22nF in series and a resistor R=180kΩ in parallel with the cell. Temperature 21°C.

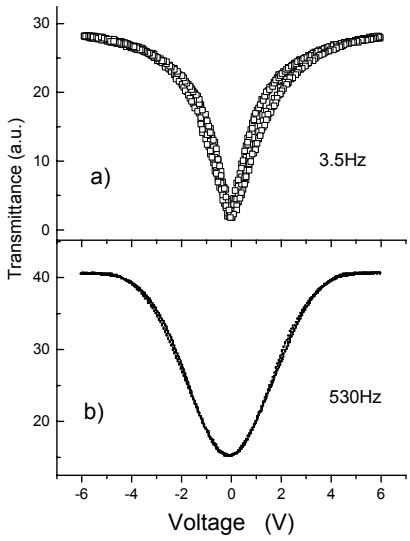

Figure 3.7: V-shaped optical transmittance of cell №2 in different regimes: a) without external elements, *f* = 3.5 Hz; b) with external capacitor C= 2.7 nF. *f* = 530 Hz:

The experiments with external capacitors allow one to measure the voltage on the FLC layer and follow the electrooptical hysteresis as a function of the voltage across that layer. Indeed, if a cell has no insulating layers at all and the voltage divider shoulder necessary for V-shaped switching is formed by an external capacitance, we can measure the same electrooptical response as a function of two different arguments, U and U_{LC}, shown in figure. 3.9.

However, to have a high contrast V-shaped response we need alignment polyimide layers, at least, one and very thin. In this case we used the cell №3 (see Table 2). In this cell the inversion of hysteresis takes place at frequency f_i=0.25 Hz. When an external capacitor C=22nF is connected in series with the same cell, a typical V-shaped switching is observed at f_i=21 Hz which is almost 100 times as without capacitor. At this frequency the aligning layer impedance may be neglected and the only reason for the V-shape electrooptical response is a change of the voltage on a FLC cell controlled solely by the external capacitor.

In figure 3.8 the external voltage U, the repolarization current oscillogram I_p and the voltage on the liquid crystal cell U_{LC} are plotted as a function of time. It is well seen that the shape of U_{LC} is quite different from U, and this difference has to modify a hysteretic behavior of the FLC layer and the shape of the current oscillograms. For example, flat peaks of I_p seen in figure 3.8 are very similar to those reported, e.g., by Chandani *et al*. [Chand].

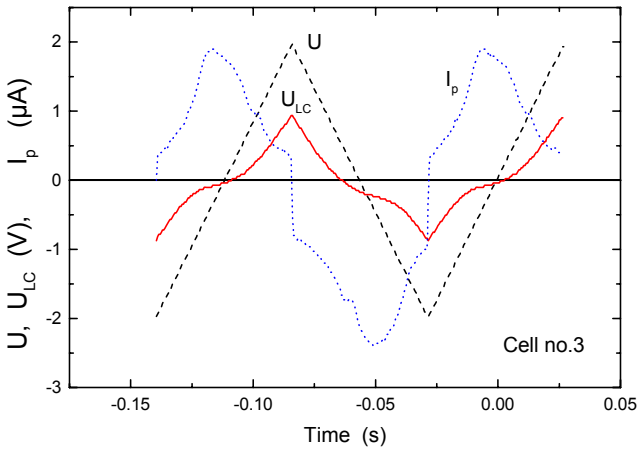

Figure 3.8: Voltage applied to the cell U, voltage on the FLC layer U_{LC}, repolarization current I_p. Cell №3. External capacitor C=22 nF.

Now, we can plot the same optical transmission in different co-ordinates, namely, as a function of the total voltage U, and as a function of the voltage on the liquid crystal cell U_{LC}, see figure 3.9.

As seen, a typical V-shaped form is observed only when the optical transmittance $T(U)$ is plotted as a function of the total voltage applied to the circuit including capacitor C, however, a hysteresis typical of conventional FLC is clearly seen in the curve $T(U_{LC})$. The latter is slightly asymmetric because the cell has only one alignment layer. Note, that the voltage on the FLC layer is considerably reduced with respect to the total voltage and this is a price which one should pay for the hysteresis-free V-shaped electrooptic switching. The same result has been obtained for several other cells having insulating layers of different thickness.

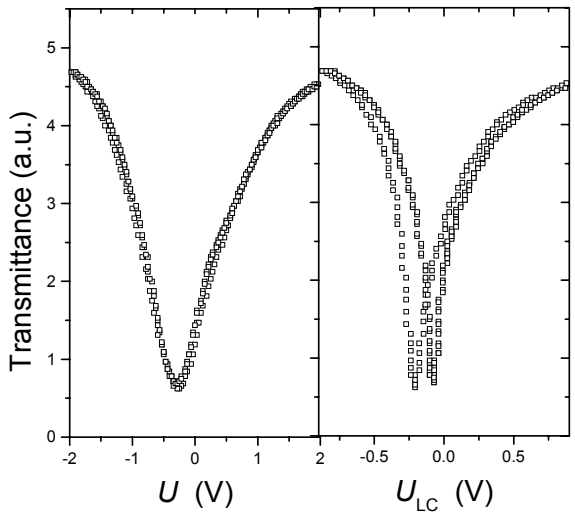

Figure 3.9: Some optical transmittance of the cell in different co-ordinates, namely, as a function of the total voltage $T(U)$, and as a function of the voltage on the cell №3, $T(U_{LC})$

The possibility to control f_i over an enormous frequency range without any change in orientation and anchoring conditions for the FLC material shows that the latter conditions are factors of minor importance for the hysteresis inversion frequency, but they can modify the general performance of the V-shaped cells, e.g. the contrast, saturation voltage, *etc*.

3.2 Dependence of the V-shaped switching parameters on the thickness of the FLC and alignment/ insulating layers

In the previous paragraph, the crucial role of the dynamic voltage divider formed by a FLC cell components, namely, the FLC and alignment layers, was demonstrated. Using external electrical elements, their performance was dramatically enhanced.

In this paragraph, we will demonstrate that optimization of the FLC and alignment layers thickness leads to the same results as utilization of an external capacitor.

3.2.1 Dependence of the inversion frequency on the alignment/insulating layer thickness. Experiment.

The capacitance, which is necessary for the operation of the voltage divider, can be created in two ways. First of all, one can fabricate by spin coating a polyimide layer with optimized thickness. From the first glance, this process should be very easy, because one can choose the optimal velocity of the spin-coater resulting in the required film thickness. This thickness can be varied from 10 nm to 150 nm. However, when the alignment layer is too thick, its surface is rough which results in bad alignment of the FLC's. On the other hand, the capacitance also depends on the dielectric constant of the polyimide, which usually is between ε_p = 3 to 4.

The other way to change the internal capacitance is to utilize dielectric films. For instance substances as Al_2O_3 , SiO_2 *etc.* form rather thick films of good quality and have the dielectric constant $\varepsilon_p \approx 10$. Hence, these films can be considered as the most suitable candidate for substituting the polymers. The thickness of such dielectric layers can be varied in a very broad range from 10 nm to 500 nm. The only requirement which should be satisfied in this case is the high transparency of the deposited layers.

First, we will investigate the influence of the polyimide alignment layer thickness on the parameters of the V-shaped switching. For that purpose we fabricated a series of the FLC cell with the same thickness of the liquid crystal layer (1.7 μm), the same area (around 1 cm^2) but with different thicknesses of the alignment layers. The cell was filled with FLC-438 (see Table 1).

The experiment shows dependencies of the voltage coercivity and the saturation voltage of FLC cells on the thickness of alignment polyimide layers (see Fig. 3.10). Figure 3.10 shows the inversion frequency f_i=10 Hz at d_p=150nm, but U_{sat}=18V.

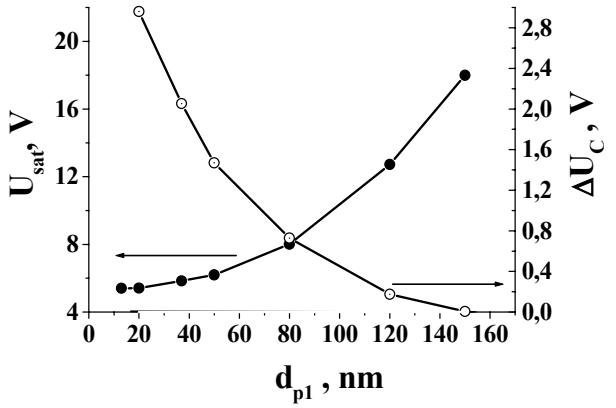

Figure 3.10: Dependencies of the saturation voltage U_{sat} and the coercive voltage ΔU_C of FLC cells (FLC-438) on thickness of alignment polyimide layers. The cell gap is 1,7μm, T=25°C, f=10 Hz

3.2.2. Dependence of the inversion frequency and saturation voltage on the FLC layer thickness

To control the capacitance of the alignment/insulating layer, a Al_2O_3 layer were evaporated over the ITO electrodes. The thickness of Al_2O_3 in these experiments was 50 nm and 70 nm. In order to align molecules of a liquid crystal, an additional thin polyimide film (10 nm) was spin-coated above the dielectric layer. The prepared substrates were utilized for assembling a wedge cell with a thickness 0,5 to 2,5 μm The cell was filled with FLC-438 (see Table 1). Replacement of polyimide layers with Al_2O_3 means increasing of ε_p and this results in diminishing the internal dielectric layers thickness which is optimal for the V-shaped switching.

The inversion frequency of that cell depends on the FLC layer thickness monotonically as it is predicted by Pikin's theory but the experiment shows a very sharp maximum in the $f_i(d)$ dependence (see Fig. 3.11). The existence of this maximum at 0,85μm allows us to obtain a very high inversion frequency. Not so

thick Al_2O_3 layers provide low saturation voltage of the V-shaped cells. Unfortunately, the reason for the appearance of such a sharp peak is not clear yet.

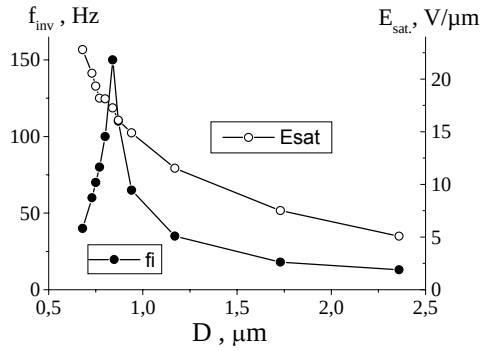

Figure 3.11: Dependencies of the inversion frequency and the saturation field of the V-shaped cell with two 70 nm Al_2O_3 insulating layers on the cell gap. Both Al_2O_3 layers are covered with 10 nm polyimide aligning layers but only one of these is rubbed. The amplitude of triangular driving voltage is ±10 V, T=35°°C, FLC mixture - FLC-438.

3.2.3 Dependence of hysteresis inversion frequency on FLC layer thickness. Computer modeling.

Experiments carried out with wedge formed cells showed that, with decreasing thickness from 2.5 down to 0.8µm, the frequency f_i increases one order of magnitude (see previous paragraph). In this paragraph computer modeling of the dependence of the inversion frequency on the alignment/insulating layer thickness as well as on the FLC layer thickness will be performed.

We can only model FLC cells with uniform gap. The result is shown in figure 3.12 for the material PBH-13 and the applied triangular voltage with amplitude ±10V. As cell conductivity *G* depends on *d.* The specific conductivity (but not G) of the material was fixed at $\sigma=10^{-9}$ (curve 1) and $\sigma=2\cdot10^{-8}Ohm^{-1}m^{-1}$ (curve 2) in Figure 3.12. The other measured parameters were as follows: cell area $S=1cm^2$, $P_s=1.2\cdot10^{-3}C/m^2$, $\Theta=34deg$, $\gamma_2=0.6Pa.s$, $p=0.2\mu m$, optical anisotropy $\Delta n=0.195$ ($\lambda=633nm$), at $T=40°C$, capacitance of two alignment layers $C=35$ nF.

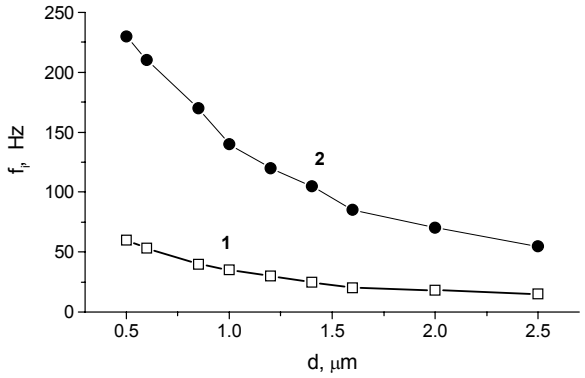

Figure 3.12: Calculated dependencies of hysteresis inversion frequency on the FLC layer thickness for two different specific conductivity of PBH-13 (40°C) mixture, $\sigma=10^{-9}$ and 2.10^{-8} $\Omega^{-1}m^{-1}$.

However, in addition to the listed parameters some others have been taken for the calculations: Frank elastic moduli $K_{1,2,3}$=15, 3 and 6 pN, respectively; compression modulus K_4=5MPa (values higher than 5MPa only weakly influence the results of calculations but increase the calculation time); the viscosity ratio $R=\gamma_{1,3}/\gamma_2=3$, ordinary refraction index n_0=1.53 (typical value for these materials); background dielectric constants ε_i=3 and typical values of azimuthal and non zenithal anchoring energy W_a=0.05 and W_z=0.5mJ/m^2. The smectic layer normal was assumed to be parallel to the substrates (bookshelf structure) because tilted layers are hardly compatible with good V-shape form of the $Tr(U_{tr})$ curve.

From figure 3.12 it is well seen that the high frequency V-shaped transmission should be observed in thin cells filled with a high conductive material. Indeed, thin cells filled with FLC-438 mixture manifest thresholdless behavior at frequencies of the order of 100Hz. An example is shown in figure 3.13 (curve 1). In this case, the voltage is ±5V (f=95Hz), the cell thickness and temperature are 0.85 μm and 30°C. The experimental curve has been modeled with the FLC-438 parameters taken at 30°C: S=1cm^2, P_s =0.82·10^{-3}C/m^2, Θ=26deg, G=4μS, γ_2=1.2Pa.s, p=0.2μm, optical anisotropy Δn=0.195 (λ=633nm), capacitance of two alignment layers C=35nF and other parameters listed in the previous paragraph. The only fitting parameter is the maximum transmission of the experimental cell (at level 0.046 predicted by modeling). The result of calculation is shown in figure 3.13

(curve 2). The two curves (1 and 2) are similar (see Fig. 3.13), however, due to some texture inhomogeneities the full darkness is not reached at the minimum of the experimental curve (the contrast is not very high, less than 10).

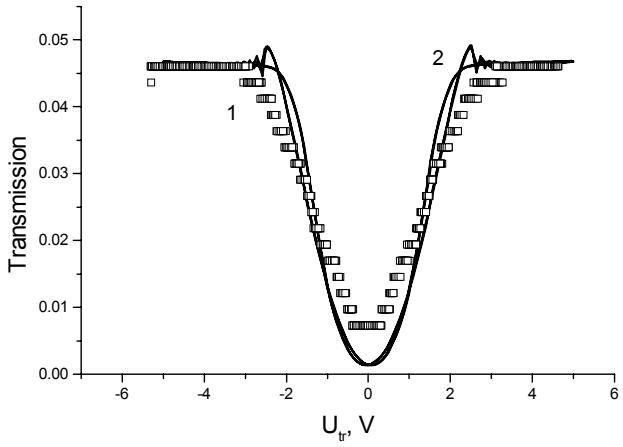

Figure 3.13: Experimental (1) and calculated (2) optical transmission curves of 0.85μm thick cell filled with FLC-438 (30°C) as function of triangular voltage ±10V, f=95Hz. Other parameters are specified in the text

3.2.4 Dependence of threshold voltage and inversion frequency on alignment layer thickness. Computer modeling.

This dependence was calculated for PBH-13 material for which the V-shaped switching is found in the range 100-200Hz and even higher, depending on the conductivity. All parameters are the same as in the previous paragraph, but the cell conductivity is assumed to be G=5μS. At f_i the distance between the two transmission minima, that is the double threshold voltage $2U_{th}$, is exactly zero. In our case, for C=35nF the frequency f=200Hz is close to the genuine inversion frequency, therefore, if we fix the frequency at 200Hz and vary C, the function $2U_{th}(C)$ would pass through the zero point at some values of C close to 35nF. In fact, it happens at C_0=44nF. It is more instructive, however, to plot $2U_{th}$ as a function of the thickness of a PI aligning layer deposited on each of the two ITO surfaces and having ε=3.75. Evidently such a curve should have a minimum at $d_p(0)=\varepsilon\varepsilon_0 S/2C_0$=37nm. Indeed we see the zero point in curve (1) plotted in figure

3.14. At the same time the genuine inversion frequency ($U_{th}\equiv 0$ at f_i) grows systematically with increasing thickness d_p, see Insert to figure 3.14. With thick layers it is possible to reach very high values of f_i at the cost of the enhanced voltage across a cell because the voltage on a FLC layer dramatically decreases with d (curve 2 in Fig. 3.14). It is interesting that for $d_p > d_p(0)$ and fixed f=200Hz< f_i the threshold voltage U_{th} is of the order of 0.1V over a wide thickness range and the $Tr(U_{tr})$ curve still has a shape similar to the V-letter with some *abnormal* hysteresis hardly to see. For $d_p < d_p(0)$ the *normal* hysteresis is observed.

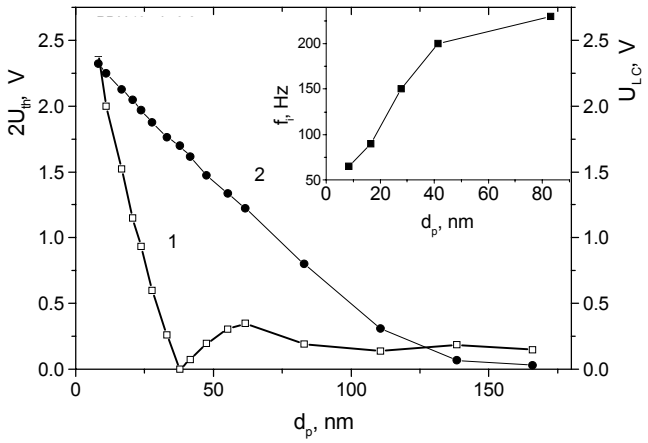

Figure 3.14: Calculated dependencies of the double threshold voltage applied to the cell at $2U_{th}$ (curve 1) and the voltage on the PBH-13 (40°C, G=5μS) layer (curve 2) as functions of the alignment layer thickness d_p. Insert: dependence of the hysteresis inversion frequency on d_p

3.3 Role of the FLC layer conductivity in V-shaped switching

In the previous paragraphs we demonstrated that the dynamic voltage divider plays an important role. However the following questions are still open:

(i) Should a V-shape switching material be necessary antiferroelectric or based on some frustrated ferroelectric structure?;

(ii) Must the spontaneous polarization indeed be large as it is assumed in the "block" model?

(iii) Is the polar anchoring energy important for the hysteresis-free switching?

(iv) How does the conductivity of an FLC influence the frequency of the hysteresis-free switching?

(v) How does a chevron structure influence the hysteresis free switching?

3.3.1 Temperature dependence of the inversion frequency

As follows from figure 3.4, a resistor connected in parallel to a FLC cell, dramatically increases f_i. Therefore, the same effect should be achieved by a change in resistance of the FLC layer. It can be done using a variation of temperature even without an external capacitance, just in the FLC configuration typical of the V-shaped switching (i.e., with alignment layers). For a new experiment we have made the cell №4 (see Table 2). The dynamic resistance of the FLC was measured using the repolarization current oscillogram *at the hysteresis inversion frequency* with the same triangular voltage form and amplitude as used for the f_i measurements.

At each temperature in the range of the smectic C* phase we found the FLC conductivity and the inversion frequency. Upon increasing the temperature from 24°C to 85°C the FLC layer conductance $G_{LC}=1/R_{LC}$ increased from 0.01 to 4.4 μS, correspondingly the hysteresis inversion frequency increased from 0.12 to 72 Hz. Evidently, f_i follows the increase in G_{LC} over the whole smectic C* phase. It is well seen in figure 3.15 where f_i is plotted as a function of specific conductivity $\sigma=G_{LC}d/S$.

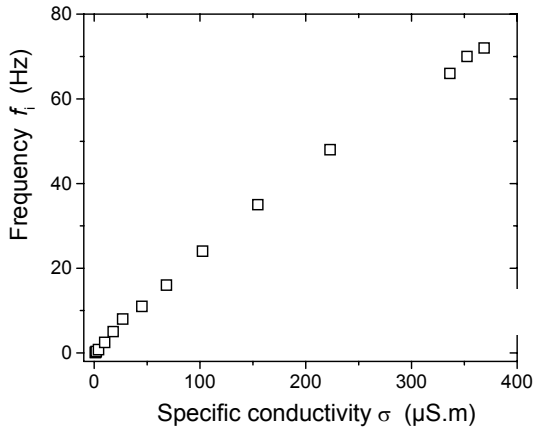

Figure 3.15: Hysteresis inversion frequency f_i as a function of specific conductivity σ for cell №4

The dependence f_i (σ) is intermediate between the linear one and the square root dependence predicted from Pikin theory. The deviation from the theory can be explained by violation of the assumption of large enough specific conductivity at low temperature. However, our results unequivocally show that the main process which controls the hysteresis inversion frequency**,** at which the true electrooptical V-shaped switching is only observed, is just a specific voltage distribution between the alignment layers and the FLC layers. The voltage divider is mostly determined by the capacitance of an insulating layer C_p and the resistance of an FLC layer R_{LC}.

3.3.2 Ionic FLC layer materials

The other possibility to vary the FLC conductivity is doping this material with some dopant.

Here we present our experimental and computational results on electrooptical switching in a commercial FLC material (FELIX-015/000 (see Table 1)) having a very small P_s value, introduced into commercial EHC cells with thin alignment layers. In such cells the V-shaped switching is usually not observed, at least, at frequencies exceeding $f \approx 1$ Hz. At $f > 1$ Hz the V-shaped switching is even not observed when the FELIX-015/000 material is slightly doped with a well

controlled impurity. However, when the same material is strongly doped with the same impurity, its conductivity markedly increases and the hysteresis-free switching is observed over a wide range of applied voltages and frequencies.

This material has a residual electric conductivity σ in the range of $(0.5\text{-}2)\cdot 10^{-9}\ \Omega^{-1}m^{-1}$ (measured in a standard 2μm thick EHC cell at T=30^{o}C with a triangular form voltage U_{tr}=5V at frequency f=1Hz). Its voltage and temperature behavior was somewhat irregular. Upon doping the electric properties of the material were stabilized.

This mixture was doped with tetracyanoquinondimethan (TCNQ) which is known as one of the best electron acceptors. The FLC and TCNQ were dissolved in acetone and obtained their uniform mixture after evaporation of the solvent at slightly elevated temperature (the homogeneity of TCNQ solutions in Felix-015/000 was checked under a microscope).

The concentration of the dopant was 0.01 wt% and 1 wt%. The phase transition temperatures of the mixtures were measured using texture observations with an electric field applied to a cell. With an accuracy of the Mettler stage of about 1^{o}C we could not notice any change in the phase transition temperatures up to c=1%. The spontaneous polarization and the tilt angle measured at T=30^{o}C show no dependence on dopant concentration, however, the electrooptical studies display a 1.4 times increase in the viscosity γ_{φ} for 1% TCNQ doped samples.

In this experiment two standard 2 μm thick EHC cells of the area 4x4mm^2 with 30$\pm$10nm thick aligning polyimide layers (data of the manufacturer) were utilized. They were filled with the FLC in the isotropic phase. The temperature dependencies of the electrical current through the cells and the electrooptical response were measured using a set-up described in the beginning of this chapter.

In the SmC* phase both the slightly and strongly doped materials show optical textures with characteristic zig-zag defects indicating the chevron-type structure, see figure 3.16. Such chevrons are spontaneously formed on the transition from the SmA phase to satisfy a strong planar anchoring at the electrodes (see Fig. 3.16).

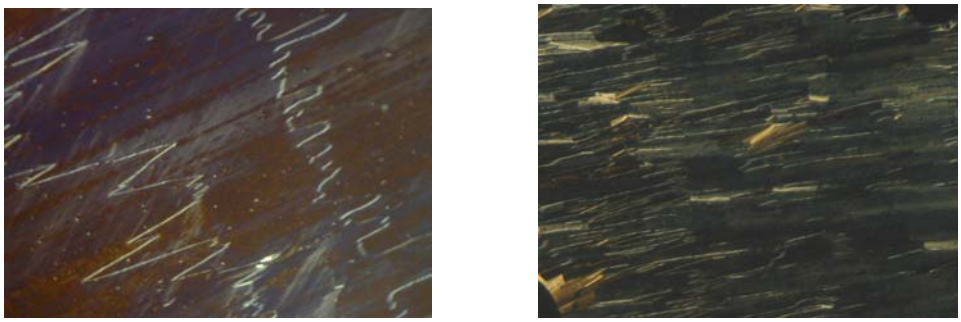

a b

Figure 3.16: Texture of the SmC* phase observed in 2 μm cells filled with Felix –015/000 mixture a) slightly doped (0.01%) and b) strongly doped (1%)

3.3.2.1 The current oscilograms. Resistivity of the cells. Experiment and computer modelling.

The current oscillograms of the two cells taken at 30°C with a voltage U_{tr}=5V at f=1Hz are shown in figure 3.17 a. For small dopant concentration (c=0.01%) the peak originated from P_s switching is well seen, the calculated value of P_s =9nC/cm^2 coincides with the Clariant data. The steps of the current corresponding to the voltage peaks allows us to find the background dielectric constant (not related to the polarization switching), ε=5.6. The ohmic conductivity of the cell filled with c=0.01% TCNQ calculated from the linear slope of the pedestal under the peak is quite small, G=0.003μS (specific conductivity σ = 0.35·10^{-9} Ω^{-1}m^{-1}. Upon further doping the conductivity increases and reach the value of G=0.02μS (σ = 2.5·10^{-9} Ω^{-1}m^{-1}) for c=1% TCNQ. In this case, the ionic current pedestal is no longer linear and the polarization peak is strongly blurred, although no change in the electrooptical switching has been noticed.

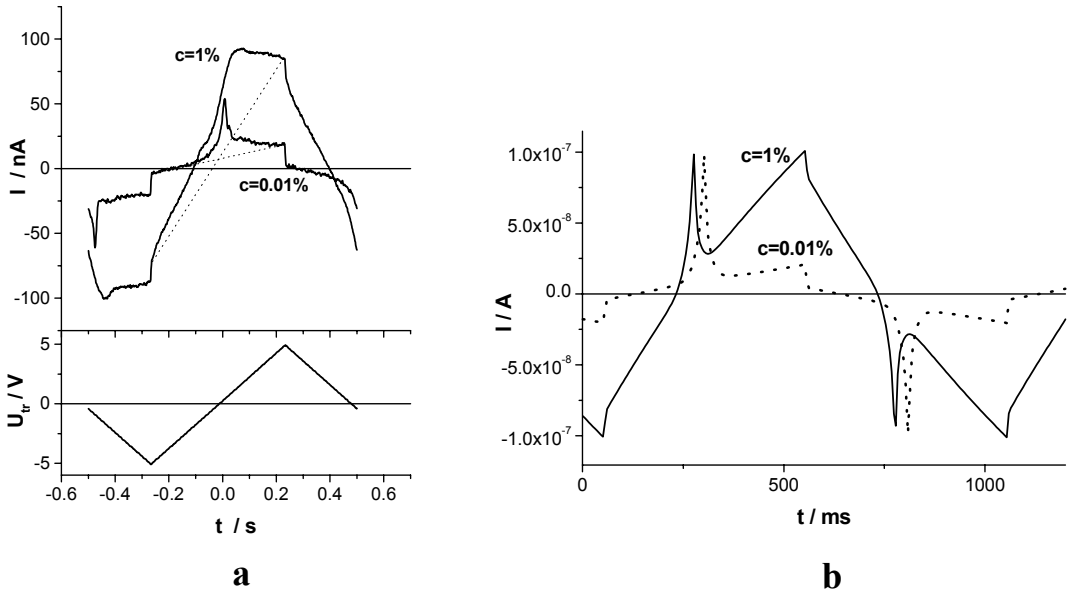

Figure 3.17: a) The current oscillograms of two FLC cells doped with small (0.01 wt %) and large (1%) concentration of TCNQ. Data are taken at 30°C with triangular voltage U_{tr}=5V at f=1Hz;
b) Calculated current oscillograms for two FLC cells filled with slightly conductive (G=0.003μS) and strongly conductive (G=0.02μS) material. Other parameters correspond to FELIX-015/000 mixture at 30°C. Calculations have been made for a symmetric chevron structure and a triangular voltage U_{tr}=5V at f=1Hz

For the slightly doped material (G=0.003μS) the experimental and calculated oscillograms (see Fig. 3.17 b) are very similar: the height and the slope of the pedestal are the same, the area under the P_s peak is also the same, P_s=9nC/cm^2. However, the calculated peak is narrower than the experimental one. We believe that it is related to the non-ideal texture of our experimental cell. At least, when the current peak coming from P_s is calculated for the bookshelf geometry, it is even narrower than that for the chevron structure shown in the oscillogram.

The discrepancy between the experiment and calculations is more serious for the strongly doped material. In experiment the conductivity current is no longer linear with the voltage and the P_s-related current peak is completely blurred. Our modeling does not show the same, the calculated current-voltage curve is linear and the P_s-related current peak on the steep pedestal is still sharp. In our opinion, two factors can be responsible for such discrepancy. First, when the electric field is applied to the real cell filled with strongly doped material the ions are no longer

distributed uniformly over the cell thickness and this may modify the current pulse shape (in our model this effect is not taken into account). The other reason can be even more serious: it is not excluded that some backflow effects which are well known for nematic liquid crystals play an important role in the smectic C* phase, especially in case of the strong conductivity. Such hydrodynamic effects are also not taken into account in the software of Dr. S Palto.

The temperature dependencies of the conductivity of the two cells are shown in figure 3.18.

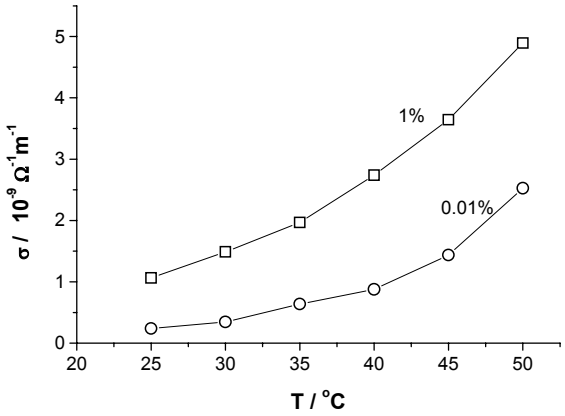

Figure 3.18: Temperature dependence of the conductivity for slightly (0.01%) and strongly (1%) doped materials (U_{tr}=5V, f=1Hz)

The increase of the conductivity $\sigma = qn\mu$ with increasing temperature is quite natural because the ion concentration n grows due to a more efficient ionization of the neutral TCNQ-FLC complexes and the ion mobility μ also grows due to a decrease in the viscosity (q is ionic charge).

In the next paragraph, we will see how this difference influences the electrooptical behavior.

3.3.2.2 Electrooptical properties of the conductive cells. Experiment and computer modeling

The field induced optical transmission $T(U_{tr})$ is measured with a cell placed between crossed polarizers in the symmetric angular position such that the transmission is a maximum for the maximal positive and negative fields. In this

case, a $T(U_{tr})$ curve has either a W-shaped with two minima or a V-shaped with one minimum.

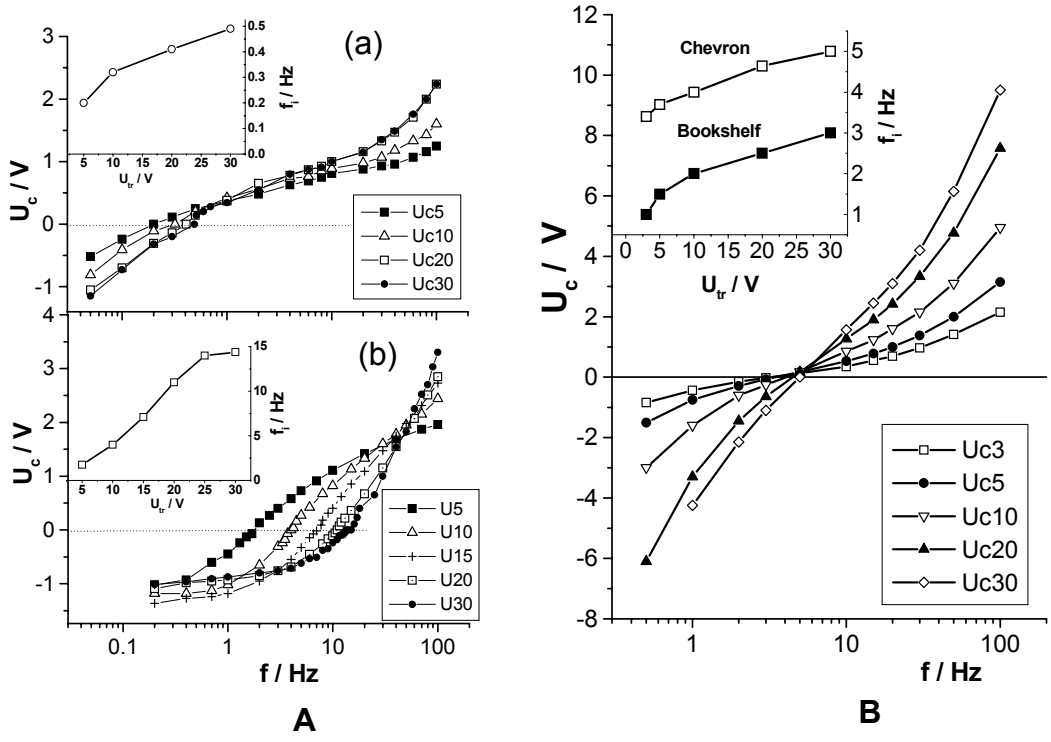

Figure 3.19: A) Frequency dependence of the coercive voltage for slightly (*a*) and strongly (*b*) doped materials. The amplitude of the applied triangular voltage is shown in the boxes. Inserts show the corresponding voltage dependencies of the hysteresis inversion frequency;
B) Calculated frequency dependence of the coercive voltage for the strongly conductive FLC material (G=0.02μS) having a symmetric chevron structure. The amplitude of the applied triangular voltage is shown in boxes. The insert shows the corresponding voltage dependencies of the hysteresis inversion frequency for the chevron structure in comparison with the bookshelf structure.

Figure 3.19 A) shows the dependence of the coercive voltage on the frequency for the same two cells described above (T=30°C). The zero line separates the areas of the abnormal (below) and normal (above) hysteresis.

For the cell filled with slightly doped material the hysteresis free V shaped switching (crossings of the zero line) is observed at very low frequency 0.2-0.5 Hz, for strongly doped sample, the inversion frequency is lying in the range 1-16 Hz

The calculated frequency dependence of the coercive voltage for the strongly conductive FLC material (G=0.02μS) having a symmetric chevron structure is shown in figure 3.19 B. The general parameters describing this mixture and the cells and utilized in calculations were taken form tables №1-2. The other parameters (at T=30°C) are the following: rotational viscosity (all three components) γ_0=0.32 and 0.45 Pa.s respectively for dopant concentration 0.01% and 1% (TCNQ), both components of the dielectric tensor ε=5.6, inverse pitch 0.01 μm^{-1}, optical anisotropy at λ=632.8nm Δn=0.155, the chevron structure was fixed by setting ϑ_1=90-ϑ=66° and ϑ_2=90+ϑ=114°. The other parameters were taken from literature for typical FLC materials: three Frank elastic moduli K_{ii}=10pN, ordinary refraction index n_o=1.53, pretilt ϑ_s=4° on both electrodes, anchoring energy 0.05mJ/m^2 (azimuthal) and 0.5mJ/m^2 (zenithal) on both electrodes, compressibility modulus was K_4= 1Mpa. We have to compare it with experimental curves shown in figure 3.19 A). In both cases, the coercive voltage passes the zero points in the frequency range centered about 4-5Hz and the shape of the curves in both cases is similar.

However, the calculated voltage dependence of the hysteresis inversion frequency is weaker than the experimental ones.

In experiments we observe hysteresis-free switching in the range f_i≈2-15Hz, the calculation results in f_i≈3.5-5.3Hz. When the calculations are carried out for the bookshelf geometry the hysteresis inversion frequency falls within the range f_i≈0.9-3Hz, see the lower curve in the Insert to figure 3.19 B). It is interesting result because a common opinion is that the V-shaped switching is hardly compatible with the chevron structures but, in fact, f_i is higher for a chevron structure. In both the bookshelf and chevron textures the calculated f_i is voltage dependent. Such a dependence comes from the voltage dependence of the switching time $\tau=\gamma_\phi/P_sE$.

The voltage dependence of f_i is shown in the Insert to figure 3.19 A): f_i is growing with increasing the voltage from 0.2 to 0.5Hz. Therefore in a standard frequency range (f >1Hz) the V-shaped switching is not seen.

Experimental investigations show that the behavior of the strongly doped material is qualitatively similar to the computer modeling but all the curves are considerably shifted to a higher frequency. It can be explained with effects like inhomogeneous FLC structure, generation of ions, which are not included in the software

Now the coercive voltage becomes zero at frequencies more than one order of magnitude higher than in the case of the slightly doped material. The inversion frequency f_i increases from 2 to 14 Hz with increasing voltage. This dependence is shown in the insert to figure 3.19 A.

The optical transmission curve taken at f_i =3.5Hz is shown in figure 3.20 a) for the triangular voltage U_{tr}=±10V. The form of the calculated V-curve for the bookshelf texture is much narrower than that for the chevron texture, and both of them are narrower than the experimental ones. The reason is, most probably, a serious inhomogeneity of the experimental textures prepared using standard EHC cells. Therefore, a voltage necessary to reach the maximum transmission (the saturation voltage) is higher for the chevron or other inhomogeneous structures than that for the bookshelf ones.

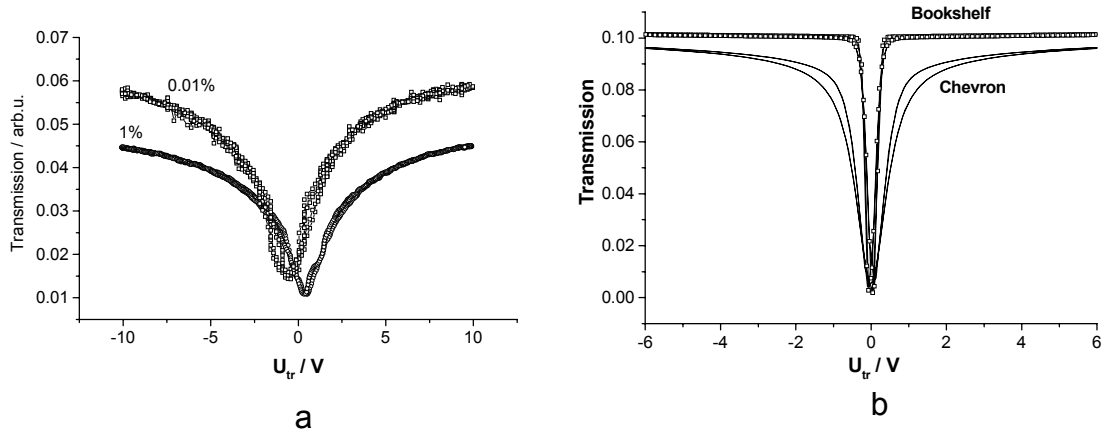

Figure 3.20: a) V-shaped optical transmittance for the 2μm thick cells filled with the slightly (*c*=0.01wt%) and strongly doped FELIX-015/000 mixture at hysteresis inversion frequencies, f_i=0.28Hz for *c*=0.01wt% TCNQ and f_i=3.5Hz for *c*=1wt% TCNQ (*T*=30°C, U_{tr}=±10V),

b) Calculated V-shaped optical transmittance for two 2μm thick FLC cells filled with the same strongly conductive (*G*=0.02μS) material but different textures, bookshelf and chevron. Other parameters correspond to the FELIX-015/000 mixture at 30°C. At U_{tr}=±10V the hysteresis inversion frequencies f_i=2Hz and =4Hz for the bookshelf and chevron structures, respectively

The voltage dependencies of the inversion frequency at three different temperatures are shown in figure 3.21. For a small concentration of ions (top plot for c=0.01%, curves for 30°C and 40°C) the inversion frequency is low (less than 0.6Hz) and almost voltage independent. With increasing the conductivity, f_i is growing and becomes voltage dependent. For the slightly doped material it reaches 2.5Hz at U_{tr}=±30V and at temperature 50°C.

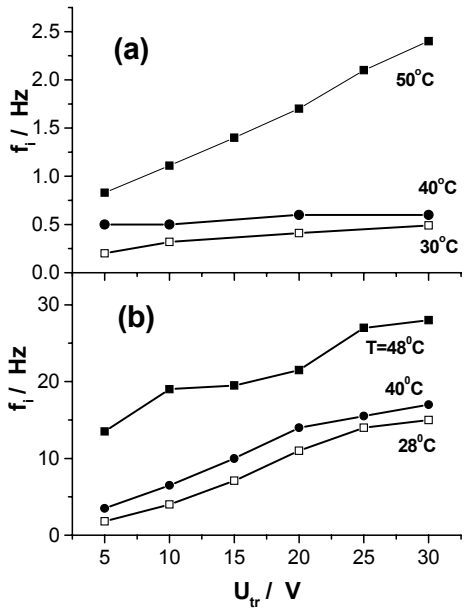

Figure 3.21: Voltage dependencies of the inversion frequency at different temperatures. *a*) slightly doped material (*c*=0.01wt% TCNQ). *b*) strongly doped material (*c*=1wt% TCNQ). Cell thickness 2 μm.

This tendency is even more pronounced for the strongly doped material (bottom plot). The maximum frequency at which the V-shape switching is observed is 27 Hz at U_{tr}=±30V at temperature 48°C. From this experiment it is quite evident that on properly doped materials one can obtain the V-shape switching at fairly high frequencies using even thin alignment layers and low spontaneous polarization.

3.4 Dependence of the inversion frequency on conductivity and spontaneous polarization. Computer modeling

In experiment, it is difficult to change one parameter not influencing the others. However, it is easy to do this by modeling. Below we vary separately the most important parameters responsible for the hysteresis-free switching: cell conductivity *G*, spontaneous polarization P_s and rotational viscosity γ_ϕ.

Calculated frequency dependencies of the coercive voltage for FLC materials having a symmetric chevron structure and different cell conductivity *G* are shown in figure 3.22. The other parameters are still the same as before. As expected, with increasing the conductivity the zero points are shifted to higher frequencies. There is, however, a very interesting curve for *G*=0. It does not cross the abscissa, but asymptotically goes to zero upon decreasing the frequency. It means, that the V-shaped regime for non-conductive FLC materials can be observed only at zero frequency. Therefore, for the V-shaped switching at any finite frequency an FLC material must be conductive.

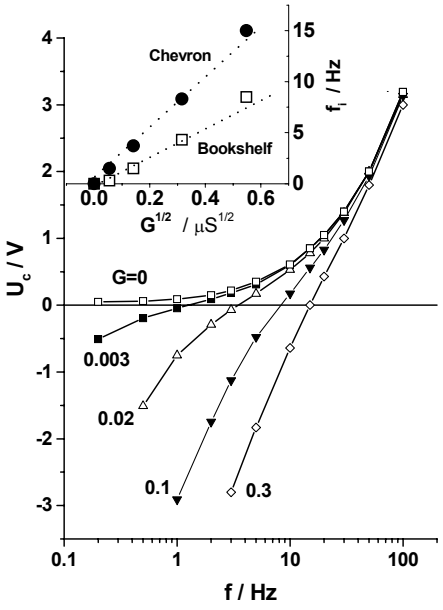

Figure 3.22: Calculated frequency dependence of the coercive voltage for the FLC materials having a symmetric chevron structure and different cell conductivity *G* shown at the curves (U_{tr}=±5V, cell thickness 2μm, area 16mm^2, other parameters correspond to FELIX-015/000 mixture at 30°C). The insert shows the corresponding dependencies of the hysteresis inversion frequency for the chevron structure in comparison with the bookshelf structure on the square root of conductivity

The dependence of hysteresis inversion frequency on the square root of conductivity is shown in the insert to figure 3.22 for both the chevron and bookshelf textures. The abscissa is selected in order to check a prediction of the simple analytical theory developed by Pikin . Indeed, the functions f_i ($G^{1/2}$) are almost linear, as predicted.

The same theory correctly describes the $f_i(C_p)$ dependence. For small P_s it also predicts a linear increase in f_i with increasing spontaneous polarization and a decrease in f_i with increasing rotational viscosity. Now we can verify that analytical result by modeling.

In this case, we model a cell with the same geometry as before, a bookshelf texture and parameters more suitable for the high frequency V-shaped switching. The capacitance of aligning layers and conductivity are close to the optimum, C_p =5nF, G=0.015μS, the rotational viscosity values are typical, γ_0=0.25 and 0.6 Pa.s. The calculated dependencies of the hysteresis inversion frequency on the spontaneous polarization for the two γ_0 are shown in figure 3.23. Indeed, for P_s<40nC/cm^2, f_i grows almost linearly with P_s and then somewhat faster. In this sense, high values of P_s are preferable for V-shape switching, however, the hysteresis-free switching is also possible for very small P_s. Low viscosity is also favorable for the fast V-shaped regime in the range of P_s<100nC/cm^2.

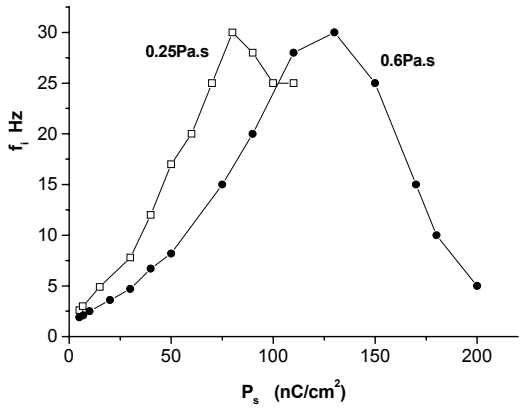

Figure 3.23: Calculated dependencies of the hysteresis inversion frequency on the spontaneous polarization for an FLC cell with the bookshelf structure. The material and cell parameters are: K_{ii}=10pN, ϑ=24deg, ε_{ii}=3.5, G=0.015μS, C_p=5nF, d=2μm, A=16mm^2, U_{tr}=±10V. The two curves are differing by the values of rotational viscosity γ_0 shown at the curves

However, with further increasing P_s the curves reach their maximum and then f_i decreases. The reason for this is not clear, but such a tendency should be taken into account when tailoring new materials for the V-shaped mode.

Chapter №4

Light modulators based on the thresholdless switching electrooptical mode

In chapter №3, we demonstrated that the capacitance of the alignment/insulating layers and the conductivity of the FLC layer play a dominant role in the thresholdless switching mode. In this chapter based on the obtained results we will show that it is possible to construct a high frequency modulator with the low saturation voltage. It will be shown that this modulator demonstrate the gray scale capabilities at frequencies which are much higher then the inversion frequency. Such behavior will be explained in the framework of the Dynamic Voltage Divider model.

4.1 High frequency V-shaped modulator

For construction of the modulators, we took the ITO coated substrates with Al_2O_3 insulating layers. In this case, the insulating layers play the role of the capacitor. The thickness of Al_2O_3 layers was 50 nm and 70 nm. Using them we constructed two cells with gaps 0.85 μm. The two cells were filled with FLC-438 (see Table 1)

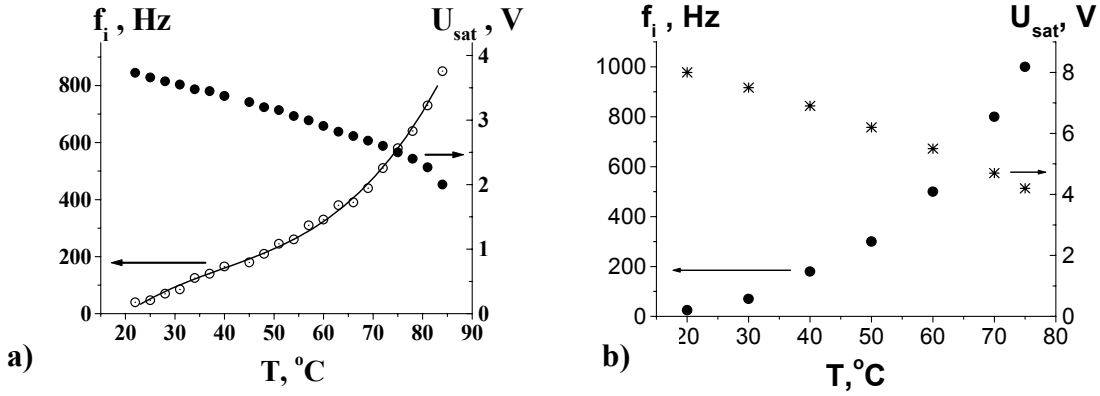

Figure 4.1: Temperature dependencies of the hysteresis inversion frequency and the saturation voltage of V-shaped cells based on FLC-438 with Al_2O_3 layers onto ITO elecrodes, FLC-layer thickness is 0.85 μm: a) Al_2O_3 layers thickness is 50 nm, one of Al_2O_3 layers is covered with the rubbed polyimide, the applied triangular voltage amplitude is ±5V, b) Al_2O_3 layers thickness is 70 nm, one of Al_2O_3 layers is covered with the rubbed polyimide, the applied triangular voltage amplitude is ±10V.

The cells were driven by the triangular voltage with an amplitude 10 V. The temperature dependence of the inversion frequency and the saturation voltage are demonstrated in figure 4.1

The inversion frequency of the cell with the Al_2O_3 layers thickness 50nm at room temperature is around 40 Hz, and the saturation voltage is less than 4V, (see Fig. 4.1a). At high temperature, near the phase transition ($T=75^0C$), the inversion frequency is equal to 600 Hz, and the saturation voltage is 2,5V. If the Al_2O_3 layer thickness is 70nm, then at room temperature f_i=15Hz, U_{sat} > 8V, and at 75°C f_i=1000Hz, U_{sat} = 4,2V (see Fig. 4.1b). These values of the inversion frequencies are the highest whenever achieved.

One can also see from these plots that the dependence of the saturation voltage is rather smooth, which is important for applications where the influence of the temperature on the performance of the modulators should be as low as possible,

4.2 Gray scale capabilities of the high frequency V-shaped modulator

To test the gray scale capabilities of the V-shaped switching cells, we selected the cell with the thickness of the Al_2O_3 layers - 50nm (see previous paragraph). The voltage applied to the cell is demonstrated in figure 4.2 (bottom curve). This voltage was generated by the programmable frequency generator. The duration of each pulse was 30 μS. In the top curve of the figure 4.2 a, one can see the electrooptical response. It is evident that the transmittance strongly depends on the amplitude of the applied pulses. So that, we can conclude that the high frequency V-shaped cell has the gray scale capabilities.

In the same time, the other interesting phenomenon was observed. Namely, if we look at the electrooptical response (see Fig. 4.2 b), it is easy to see that the response time of our cell under these conditions is around 8μs and the cell does not show bistability at this time scale. Such a strange behavior , at first glance, allowed to have gray scale

In the same time, it is known from our previous measurements the response time of FLC-438 should be much slower. What is the reason? The explanation of this phenomenon see in the forthcoming paragraph.

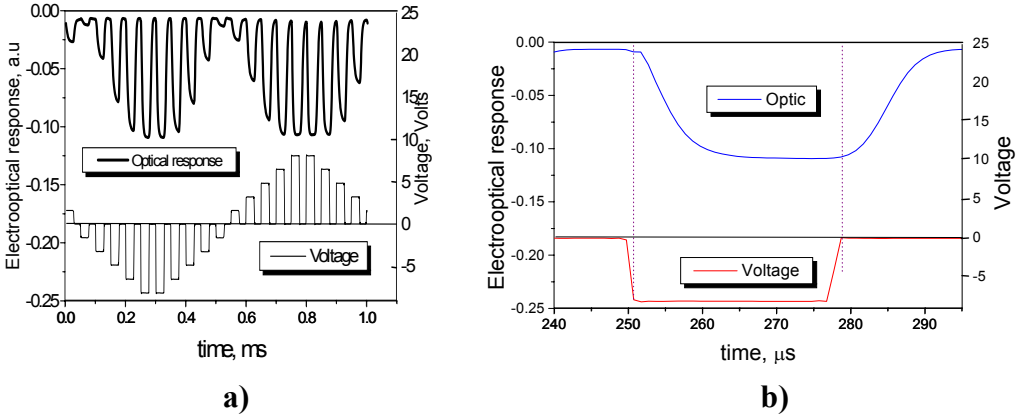

Figure 4.2:: a) the driving voltage waveform (bottom curve) and the electrooptical response of a V-shaped cell (top curve). Pulses are 30μs long. b) zoom of the driving voltage waveform (bottom curve) and the electrooptical response of a V-shaped cell (top curve). T=30°C

4.3 Response to polar pulses with high duty ratio

In the previous paragraph, it has been found experimentally that FLC cells with thick aligning layers do not show bistable response to polar pulses of high duty ratio. What is quite specific is a fast relaxation of the field off state (no memory effect).

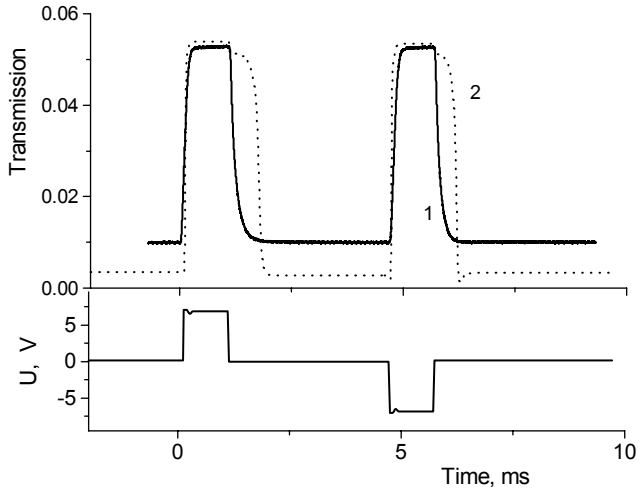

Figure 4.3 : Experimental (1) and calculated (2) oscillograms of electrooptical response of 0.8μm thick cell filled with FLC-438 (30°C, *G*=1μS) to polar voltage pulses shown at the bottom

For modeling the same parameters were used as before for this mixture with the same capacitance (C=35nF) of the alignment layers. The calculated curve 2 in figure 4.3 decays slower than curve 1, however its main feature is the same (no memory). It looks like the back relaxation of FLC is accelerated by a field of opposite sign with respect to the pulse polarity.

Such a field should be provided by a discharge of capacitance *C* through the external circuit after the end of the pulse from a function generator. This is exactly what our modeling shows (see Fig. 4.4).

We increase the capacitance *C* from 27 to 1000nF/cm^2 (curves 1-5) and follow a change in the cell transmission (top) and voltage on the FLC layer (bottom). This increase of capacitance is equivalent to a decrease of the thickness of an aligning PI layer from 60nm to 1.6nm. Curve 1 in the bottom plot clearly indicates that, after the positive voltage pulse, an inverse (negative) voltage remains on the FLC layer for about t_{inv}=0.5 ms. This inverse voltage forces the optical transmission to vanish very fast, within the same 0.5 ms (curve 1 on the top plot). With increasing the capacitance (curves 1$\rightarrow$5), the t_{inv} time increases, the delay in the optical transmission pulse become longer, and finally, in the limit of infinitely thin aligning layers ($C\rightarrow\infty$) the voltage on the FLC layer repeats the shape of the external voltage pulse and the optical response manifests the true bistability (curves 5 on both plots). Experimentally we have checked this trend using a standard 2μm thick cell with thin aligning layers and several *external* capacitors connected in series with the cell. The results of our calculations have completely been confirmed. Therefore, our modeling has resulted in a better understanding of the nature of two relevant phenomena, the V-shaped switching and bistability. In fact, they are two sides of the same medal. With a large capacitance and/or high conductivity of alignment layers, the inverse field is very low and true bistability is observed. On the contrary, with a small capacitance and low conductivity of aligning layers (and also with enhanced conductivity of an FLC) the V-shape electrooptical switching is observed.

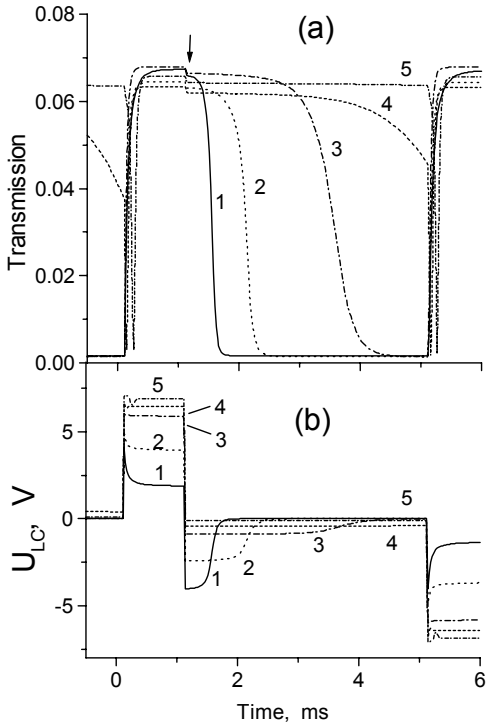

Figure 4.4: Calculated oscillograms of optical transmission (a) and voltage on the FLC layer (b) for 0.8μm thick cell filled with FLC-438 (30°C, *G*=1μS). The capacitance of aligning layers is varied: *C*=27 (1), 35(2), 100(3), 200(4) and 1000 nF/cm^2 (5)

Conclusion

The main aim of the present work was the investigation of the mechanism of the thresholdless hysteresis free electrooptical mode – V-shaped mode - in the chiral smectic C* phase of Ferroelectric Liquid Crystals.

As it was shown in the chapter №1, despite all affords the physics of this effect was unclear until the beginning of this thesis.

The present work was based on the assumption that the crucial factor for the V-shaped mode is a form of the electric field applied to the FLC layer. Such a specific electric field is the consequence of the dynamic voltage divider formed by the alignment/insulating layers and a FLC layer.

To prove this hypothesis, experimental and computer modeling techniques were utilized.

In the experiments we investigated a number of FLC mixtures which parameters (spontaneous polarization, viscosity, tilt angle, response time) are varied in a broad range. This was to demonstrate that the V-shaped mode is a general effect in FLC's and , namely, the dynamic voltage divider plays a crucial role.

First, we demonstrated that the FLC cell is real dynamic voltage divider. For that purpose it was demonstrated that the capacitance of the FLC layer of the standard cell filled with the mixture Felix 015/000 (Clarian) decreases at more than 10 times upon the application of the external electric field, whereas other parameters (mainly resistivity of both of the layers) are constant. To confirm our assumption about the role of the dynamic voltage divider, we modeled its electrical parameters by attaching external elements a) the capacitor in series to modify the alignment layers capacitance and b) the parallel resistivity to modify the FLC layer conductivity. As a result, we observed the dramatic increase of the value of the inversion frequency. In addition the external capacitance allowed us to measure the voltage applied to the FLC layer. As it was expected, this voltage has a different form and amplitude than the total one. When we plotted the electrooptical response as a function of this voltage on one side and the total voltage on the other side we saw that the electooptical response is really thresholdless and hysteresis free, but only for the latter case. For the former one

it has a typical hysteresis loop. It means that the V-shaped switching is rather apparent but not a real effect.

The further investigations were implemented in order to understand the role of the parameters of the cell (FLC and alignment/insulating layers thickness) for the performance of the V-shaped mode.

For that purpose, we fabricated the wedge FLC cell filled with FLC 438 and having the Al_2O_3 insulating layers. It was shown that the dependence of the inversion frequency on the FLC layer thickness had two distinguished regions: a) from 0.8 μm to 1.8 μm, this function went down as it was predicted by the Pikin theory, b) from 0.6 μm to 0.8 μm it increased, this can be explained by the local variation of the parameters of the cell. During the same time, the saturation voltage gradually decreases, which was also in accordance with Pikin's theory. Moreover, the computer modeling confirmed these experiments.

The influence of the FLC conductivity on the V-shaped mode was investigated in detail. First, we selected the FLC mixture with low spontaneous polarization (Felix 015/000) and a thick commercially available EHC cell (2 μm). According to any previous theory, the existence of the V-shaped under these conditions is impossible. After that, this mixture was doped with TCNQ at two different concentrations (0.01% and 1 %) and infiltrated in the cells.

Our experiments showed that the inversion frequency for the strongly doped mixture is ten times higher than that for slightly doped one and it is equal to 26 Hz. This result proves that the conductivity of the FLC's plays a crucial role in the V-shaped switching. Computer modeling also confirmed this result.

Finally, it was demonstrated that the V-shaped mode has really a gray scale capabilities.

The future work in this field should be connected with investigation of the influence of the physical parameters of the FLC mixtures, alignment layers conductivity on the performance of the V-shaped mode as well as the adaptation of this electrooptical mode for utilization in FLC-microdisplays.

Zusamenfassung (auf Deutsch)

Die Hauptaufgabe der vorliegenden Arbeit bestand darin, den Mechanismus des schwellspannungsfreien und hystereselosen elektrooptischen Schaltmodus, auch V-förmiger Schaltmodus genannt, der in der chiralen smektischen C* Phase (das sind ferroelektrische flüssigere Kristalle, FLC's) auftritt, zu untersuchen.
Wie in Kapitel 1 gezeigt wurde, war die Physik dieses Effektes trotz mehrerer vorher publizierter Arbeiten am Beginn dieser Dissertation unklar.
Die vorliegende Arbeit basiert auf der Annahme, dass der bestimmende Einfluß auf das Vorliegen des V-förmigen Modus eine spezifische Form des elektrischen Feldes ist, das auf die FLC Schicht wirkt. Solch ein spezifisches elektrisches Feld ergibt sich als Konsequenz aus dem dynamischen Spannungsteiler, der aus den Isolierschichten und der FLC Schicht besteht.
Um die Gültigkeit der zugrundeliegenden Ausgangsüberlegung zu überprüfen, wurden experimentelle Untersuchungen und Computersimulationen ausgeführt.

In die experimentellen Untersuchungen wurden eine Vielzahl verschiedener FLC Mischungen einbezogen, deren physikalische Parameter wie spontane Polarisation, Viskosität, Tiltwinkel und Schaltzeit in einem breiten Bereich variiert wurden. Es konnte gezeigt werden, dass das V-förmige Schalten im Prinzip bei allen FLC's auftritt, wobei der dynamische Spannungsteiler eine entscheidende Rolle spielt.

Am Beginn der Experimente wird gezeigt, dass die FLC Zelle die Funktion eines realen und dynamischen Spannungsteilers erfüllt.
Es wurde experimentell verifiziert, dass die Kapazität der FLC-Schicht der Standardzelle mit der Mischung Felix 015/000 (Clarian) nach der Anwendung des externen elektrischen Feldes 10 mal mehr abnahm als ohne angelegtes elektrisches Feld, während andere Parameter wie der elektrische Widerstand beider Polymerschichten konstant blieben.
Um das Modell des elektrischen Spannungsteilers zu verifizieren, wurden die elektrischen Parameter gezielt über externe Elemente modelliert A) Ein Kondensator in Reihe erlaubte die Modifizierung der Kapazität der polymeren

Orientierungsschichten; B) Ein Widerstand in Parallelschaltung erlaubte die Änderung der Leitfähigkeit der FLC's. Dadurch bedingt erreichten wir eine dramatische Zunahme der Inversionsfrequenz. Zusätzlich war es möglich, über den externen Kondensator die an der FLC-Schicht anliegende Spannung zu vermessen. Wie erwartet, hat diese Spannung eine andere Form und eine andere Amplitude als die Gesamtspannung. Beim Auftrag der elektrooptischen Antwort als Funktion einmal der an der FLC-Schicht angelegten Spannung, zum anderen der Gesamtspannung, fanden wir, daß die elektooptische Antwort nur für den Fall des Autrages als Funktion der Gesamtspannung schwellspannungsfrei und hysteresefrei ist. Im ersteren Fall, des Spannungsabfalles über die FLC-Schicht, lag ein typischer Hystereseeffekt vor. Daraus war der Schluß zu ziehen, daß das V-förmige Schalten kein realer Effekt ist.

Die weiteren Untersuchungen wurden ausgeführt, um den Einfluss der Zellparameter wie Dicke der FLC-Schicht und Dicke der Orientierungsschichten auf die Performance der V-förmigen Kurve verstehen zu lernen.
Zu diesem Zweck wurde eine keilförmige FLC-Zelle, die Isolierschichten aus Al_2O_3 enthält, mit der Mischung FLC 438 gefüllt. Es konnte gezeigt werden, daß die Abhängigkeit der Inversionsfrequenz von der FLC-Schichtdicke sich in zwei unterschiedlichen Bereichen verschieden verhält: a) Bei einer Schichtdicke zwischen 0.8 µm bis 1.8 µm nimmt die Inversionsfrequenz ab, wie dies durch die Pikin-Theorie vorausgesagt wurde, b) Der Anstieg von 0.6 µm bis 0.8 µm kann durch die lokale Veränderung der Zellparameter erklärt werden. Parallel dazu nahm die Sättigungsspannung stufenweise ab, auch dies im Einklang mit der Pikin-Theorie. Außerdem bestätigten die Computermodelle diese Experimente.
Der Einfluss der FLC-Leitfähigkeit auf den V-förmigen Schaltmodus wurde im Detail untersucht. Zuerst wählten wir eine kommerzielle Mischung-FLC Felix 015/000-mit niedriger spontaner Polarisation aus, die Zellendicke der im Handel erhältlichen EHC Zellen betrug 2 µm. Nach allen in der Literatur vorliegenden Arbeiten tritt unter diesen Bedingungen das V-förmige Schalten nicht auf. Diese Mischung wurde mit TCNQ bei zwei unterschiedlichen Konzentrationen (0.01% und 1 %) dopiert und in die Meßzellen gefüllt..

Unsere Experimente zeigten, dass die Inversionsfrequenz für die stark dopierte Mischung mit 26 Hz ca. 10mal größer ist als bei der niedrig dopierten Probe. Dieses Resultat zeigt, dass die Leitfähigkeit den entscheidenden Einfluß auf das Auftreten des V-förmigen Schaltmodus im FLC spielt. Schließlich konnte demonstriert werden, dass der V-förmige Schaltmodus tatsächlich graustufenfähig ist.

Zukünftige Aktivitäten auf diesem Gebiet sollten der Untersuchung des Einflusses der physikalischen Parameter der FLC-Mischungen und der Leitfähigkeit der polymeren Orientierungsschichten auf die Güte des V-förmigen Schaltmodus dienen. Ebenso wichtig ist die Aufgabe, diesen elektrooptischen Modus auf Anwendungsaspekte hin zu untersuchen, z.B. auf den Einsatz in FLC-Mikrodisplays.

References

[Abdulhal] I. Abdulhalim, *Opt. Comm.*, 144, 1997, pp. 169-178

[AbdulMod] I. Abdulhalim, G. Moddel, K. M. Johnson, *Appl. Phys. Lett.*, **55**, 1989, pp. 1603-1605

[BelSon] V. A. Belyakov, A. S. Sonin, Optics of cholesteric liquid crystals, Nauka, 1982 (in Russian)

[BerScha] L. A. Beresnev, V. G. Chigrinov, D. I. Dergachev, E. P. Pozhidaev, J. Fünfschilling, M. Schadt, *Liq. Crys.,* **5**, 1989. pp.1171-1182

[Blinov] L. M. Blinov, V. G. Chigrinov, Electrooptic effects in liquid crystal materials, Springer –Verlag, New York, 1994

[Blm1] L. M. Blinov, E. P. Pozhidaev, F. V. Podgornov, A. Sinha, W. Haase, *Ferroelectrics*, **277**, 2002, pp. 3-11

[Blm2] L. M. Blinov, E. P. Pozhidaev, F. V. Podgornov, S. A. Pikin, S. P. Palto, A. Sinha, A. Yasuda, S. Hashimoto, W. Haase, *Phys. Rev. E* , **66**, 2002, 21701

[Blm3] S. P. Palto, L. M. Blinov, F. V. Podgornov, W. Haase**,** *Mol. Crys. and Liq. Crys.,* in print

[Blm4] L. M. Blinov, S. P. Palto, A. L. Andreev, E. P. Pozhidaev, F. V. Podgornov, W. Haase, *Mol. Crys. and Liq. Crys.*., in print

[Chand] A. D. L. Chandani, Y. Cui, S. S. Seomun, Y. Takanishi, K. Ishikawa, H. Takezoe, A. Fukuda, *Liq. Crys*., **26**, 1999, pp. 167-179

[ChieYag] T. C. Chieu, K. H. Yang, *Appl. Phys. Lett.,* **56**, 1990, pp.1326-1328

[ClarBar] N. A. Clark, J. E. Maclennan, R. Shao, D. Coleman, S. Bardon, T. Bellini, D. R. Link, G. Natale, M. A. Glaser, D. M. Walba, M. D. Wand, X. H. Chen, P. Rudquist, J. P. Lagerwall, M. Buivydas, F. Gouda, S. T. Lagerwall, , *J. Mater. Chem*., **9**, 1999, pp. 1257-1261

[ClarCol] N. A. Clark, D. Coleman, J. E. Maclennan, *Liq. Crys*., **27**, 6, 2000, pp. 985-990

[ClarkHa] M. A. Handshy, N. A. Clark , *Ferroelectrics*, 59, 1984

[Cop] M. Čopic, J. E. Maclennan, N. A. Clark, *Phys. Rev. E,* **65**,2002, 021708

[Elston] E. E. Kriezis, L. A. Parry-Jones, S. J. Elston, Optical properties and applications of ferroelectric and antiferroelectric liquid crystals, in Optical applications liquid crystals, *Inst. Of Physics*, 2003

[Elst1] N. J. Mottram, S.J. Elston, *Liq. Crys*., 12, **26,** 1999**,** 1853-1856

[Elst1] N. J. Mottram, S.J. Elston, *Phys. Rev. E,* 5, **65**, 2000, pp. 6787-6794

[Fukuda] A. Fukuda, *Proc. of the 15th International Display Research Conference, Asia Display,* 1995

[FukudIsh] A. Fukuda, S. S. Seomun, T. Takahashi, Y. Takanishi, K. Ishikawa, *Mol. Crys. Liq. Crys Sci. Technol. Sect. A*., **303**, 1997. 378-389

[GlogPav] M. Glogarova, J. Pavel, Journ. De Physique, 45, 1984

[GorMie] E. Gorecka, D. Pociecha, M. Glogarova, J. Mieczkowski, *Phys. Rev. Lett.,* **81**, 1998, pp. 2946-2949

[Hayashi] N. Hayashi, T. Kato, T. Aoki, T. Ando, A. Fukuda, S. S. Seomun, *Phys. Rev. E*, **65**, 2002, 041714

[Inui] S. Inui, N. Iimura, T. Suzuki, H, Iwane, K. Miyachi, Y. Takanishi, A. Fukuda, *J. Mater. Chem*., **6**, 1996

[Jeu] G. Vertogen, W. H. de Jeu, Thermothropic liquid crystals, Fundamentals, Springer-Verlag, Berlin, 1988

[LagClar] N. A. Clark, S. T. Lagerwall, *Appl. Phys. Lett.*, **36**, 1980, pp. 899-901

[Lwall] S. T. Lagerwall, Ferroelectric and antiferroelectric liquid crystals, Wiley-VCH,Weinheim, 1999

[MacClar] M. Čopic, J .E. Maclennan, N. A. Clark, *Phys. Rev. E,* **63**, 2001, 031703

[Meyer] R. B. Meyer, L. Liebert, L. Strzelecki, P. Keller, *Journ. Phys. Lett.*, **36**, 1975

[Modd] G. Moddel, Ferroelectric liquid crystal spatial light modulators, 1994

[NakaIch] T. Nakamura, H. Ichinose, S. Naemura, *Jap. J. Appl. Phys.,* 26, 1987

[Ocall] M. J. O`Callaghan, *Phys. Rev. E*, **67**, 2003, 011710

[ParNak] B. Park, M. Nakata, S.S. Seomun, Y. Takanishi, K. Ishikawa, H. Takezoe, *Phys. Rev*. E, **59**, 1999, pp. 3815-3818

[ParTak] B. Park, S. S. Seomun, M. Nakata, Y. Takanishi, K. Ishikawa, H. Takezoe, *Jpn. J. Appl. Phys., Part 1*, **38**, 1999, pp. 1474-1481

[SeoGao] S. S. Seomun, T. Gauda, Y. Takanishi, K. Ishikawa, H. Takezoe, A. Fukuda, C. Tanaka, T. Fujiyama, T. Maruyama, S. Nishiyama, Dig. AM-LCD, 96, 1996

[SeoIsh] S. S. Seomun, T. Gauda, Y. Takanishi, K. Ishikawa, H. Takezoe, A. Fukuda, , *Liq. Crys*., **26**, 1999, pp. 151-161

[SeoNish] S. S. Seomun, Y. Takanishi, K. Ishikawa, H. Takezoe, A. Fukuda, C. Tanaka, T. Fujiyama, T. Maruyama, S. Nishiyama, *Mol. Crys. Liq. Crys. Scie. Technol., Sect. A*, **303**, 1997, pp. 436-447

[SeoPar] S. S. Seomun, B. Park, A.D.L. Chandani, D. S. Hermann, Y. Takanishi, K. Ishikawa, H. Takezoe, A. Fukuda, *Jpn. J. Appl. Phys.,* **37**, 1998, pp. 645-658

[SeoTak] S. S. Seomun, Y. Takanishi, K. Ishikawa, H. Takezoe, A. Fukuda*, Jpn. J. Appl. Phys.* **36**, 1997, pp. 1278-1290

[Shiba] S. Shibahara, J. Yamamoto, Y. Takanishi, K. Ishikawa, H. Yokoyama, H. Takezoe, *Phys. Rev. E*, **63**, 2001, 051707

Curriculum Vitae

Name:	Fedor V. Podgornov
Date of birth:	16 May 1972
Place of birth:	Korkino, Chelyabinsk oblast, Russia
Natinality	Russian
Family status	single
Parents:	Valery Ivanovich Podgornov (engineer)
	Nadezhda Vladimirovna Podgornova(Jurowskyh) (engineer)
1979 – 1989	Mathematical school 31, Chelyabinsk, Russia
1989 –1993	Study of optics under guidance of Prof. B.Ya. Zeldovich, Southern Ural State University, Chelyabinsk, Russia
December 1993	Diplom in Electrophysics (Dipl.-Phys)
1994- 1999	Junior Scientic Researcher at Southern Ural State University, Department of Applied Mathematics and Physics, Russia
1999-2004	PhD student of Prof. W. Haase, Institute of Physical Chemistry, Darmstadt University of Technology

This work was carried out in Institute of Physical Chemistry (Darmstadt University of Technology) under guidence of Prof. Dr. W.Haase from April 1999 till March 2004.

List of publications

[F1] N. D. Kundikova, F. V. Podgornov, B. Ya. Zel'dovich, **"Manifestation of spin- orbit interaction of a photon in a vacuum"**. *Pure and Applied Optics*, **4**, 1995

[F2] B. Ya. Zel'dovich, N. D. Kundikova, F. V. Podgornov, L.F. Rogacheva**,"Experimental obtaining a light «flash» moving with arbitrary velocity in vacuum"***, Kvantovaya Elektronika (Quantum Electronics)*, **23**,11, 1996

[F3] S. A. Podoshvedov, F. V. Podgornov**, "Two waves mixing in a cubic-nonlinear media: eigenmodes, spatial instability, and bifurcation",** *Optika i spektroskopija (Optics and spectroscopy)*, **81**, 9, 1996

[F4] N. B. Baranova, V. A. Krivoschokov, B. Ya. Zel'dovich, F. V. Podgornov**, "Liquid crystalline analizator of the state of light polarization"**, *Sov. Journal of quantum electronics*, **10**, 1997

[F5] B. Ya. Zel'dovich, N. B. Baranova, V. A. Krivoschokov, F. V. Podgornov, **"Polariscope:Theory and Experiment"**, *Molecular Crystals and Liquid Crystals*, **321**, 1998

[F6] F. V. Podgornov, I. B. Tsarev, V. A. Krivoschokov, **"Liquid crystalline compensator"**, *Molecular Crystals and Liquid Crystals*, **321**, 1998

[F7] S. A. Podoshvedov, F. V. Podgornov**, " Peculiarity of exchange among four unidirectional light waves in a nematic liquid crystal under exciting thermal static lattices: Eigenmodes, their instability, bifurcations and optical switching"**, *Molecular Crystals and Liquid Crystals*, **321**, 1998

[F7] F. Podgornov, E. Pozhidaev, D. Ganzke, W. Haase**, "Variable optical attenuator based on deformed helix ferroelectric liquid crystals"**, *Proceedings of ISAF 2000 (IEEE Catalog Number 00CH37076)*, 2000

[F8] W. Haase, F. Podgornov, **"Fast switchable devices based on ferroelectric liquid crystals**", *J. Opt. Tech.*, **68**, 2001

[F9] S. P. Palto, L. M. Blinov, F. V. Podgornov, W. Haase**," Modeling electrooptical effects in ferroelectric liquid crystals. 1. Basic equations and experimental tests",** *Molecular Crystals and Liquid Crystals,* in print

[F10] L. M. Blinov, S. P. Palto, A. L. Andreev, E. P. Pozhidaev, F. V. Podgornov, W. Haase, **"Modeling electrooptical effects in ferroelectric liquid crystals. 2. V-Shape switching in SmC* phase"**, *Molecular Crystals and Liquid Crystals*., in print

[F11] W. Haase, F. Podgornov, E. Pozhidaev, **"Polarization-insensitive modulator based on deformed helix ferroelectric liquid crystals",** *Proc. SPIE 4481*, 2002

[F12] L. M. Blinov, E. P. Pozhidaev, F. V. Podgornov, A. Sinha, W. Haase, "**Hysteresis Inversion Frequency for V-Shaped Electrooptical Switching Controlled by Dynamic Impedance of Ferroelectric SmC* Phase**" *Ferroelectrics*, **277**, 2002

[F13] L. M. Blinov, E. P. Pozhidaev, F. V. Podgornov, S. A. Pikin, S.P. Palto, A. Sinha, A. Yasuda, S. Hashimoto, W. Haase, **" "Thresholdless" Hysteresis-Free Switching as an Apparent Phenomenon of Surface Stabilized Ferroelectric Liquid Crystal Cells"**, *Phys. Rev. E* , **66**, 2002

[F14] W. Haase, S. A. Pikin, F. V. Podgornov, E. P. Pozhidaev, H. Moritake, A.D.L. Chandani Perera, **"Thresholdless hysteresis-free switchable FLC materials"**, *SPIE Proceedings*, **5003**, 2003

[F15] M. V. Kozlovsky, F. V Podgornov, G. Wang, W. Haase, **"Photoselection- Governed Holographic Grating Recording in a Chiral Side Chain Azo Dye Liquid Crystalline Polymer",** *Phys. Stat. Sol.,* **198,** 2003

[F16] L. M. Blinov, S. P. Palto, F. V. Podgornov, H. Moritake, W. Haase, **"Hysteresis- free electrooptical switching in conductive ferroelectric liquid crystals: experiments and modelling"**, *Liquid. Crystals*, 31, 1, 2004

Eidesstattliche Erklärung

Ich erkläre hiermit an Eides Statt, dass ich meine Dissertation selbständig und nur mit den angegebenen Hilfsmitteln angefertigt habe.

_____
Fedor V. Podgornov

Erklärung

Ich erkläre hiermit, noch keinen Promotionsversuch unternommen zu haben.

_____
Fedor Podgornov

Acknowledgements

- I want to express my sincere acknowledgement to Prof. Dr. W. Haase for his guidence me during this work.
- I am very gratefull to Prof. Dr. T. Tschudi for the fruitful discussions and his sincere help.
- I am also thankful to Prof. L. M. Blinov and Prof. S.A.Pikin (Institute of Crystallography, Russian Academy of Sciences, Moscow, Russia) for our fruitful joint work on the V-shaped switching in FLC's.
- My special thanks to Dr. E. P. Pozhidaev (Lebedev Physical Institute, Russian Academy of Sciences, Moscow, Russia) for our joint work in the field of Ferroelectric Liquid Crystals.
- I would like to acknowledge Dr. A. Yasuda and Dr. S. Hashimoto (Sony Corp.) for our fruitful scientific colaboration and the financial support of this work.